Journal of Medicinal Chemistry

Article

Development of Stem Cell Mobilizing Agents Targeting CXCR4 Receptor for Peripheral Blood Stem Cell Transplantation and Beyond

Chien-Huang Wu, Jen-Shin Song, Hsuan-Hao Kuan, Szu-Huei Wu, Ming-Chen Chou, Jiing-Jyh Jan, Lun Kelvin Tsou, Yi-Yu Ke, Chiung-Tong Chen, Kai-Chia Yeh, Sing-Yi Wang, Teng-Kuang Yeh, Chen-Tso Tseng, Chen-Lung Huang, Mine-Hsine Wu, Po-Chu Kuo, Chia-Jui Lee, and Kak-Shan Shia

J. Med. Chem., **Just Accepted Manuscript** • DOI: 10.1021/acs.jmedchem.7b01322 • Publication Date (Web): 09 Jan 2018

Development of Stem Cell Mobilizing Agents Targeting CXCR4 Receptor for Peripheral Blood Stem Cell Transplantation and Beyond

Chien-Huang Wu,[†] Jen-Shin Song,[†] Hsuan-Hao Kuan,[†] Szu-Huei Wu, Ming-Chen Chou, Jiing-Jyh Jan, Lun K. Tsou, Yi-Yu Ke, Chiung-Tong Chen, Kai-Chia Yeh, Sing-Yi Wang, Teng-Kuang Yeh, Chen-Tso Tseng, Chen-Lung Huang, Mine-Hsine Wu, Po-Chu Kuo, Chia-Jui Lee and Kak-Shan Shia*

Institute of Biotechnology and Pharmaceutical Research, National Health Research Institutes, Miaoli County 35053, Taiwan, R.O.C.

ABSTRACT:

The function of the CXCR4/CXCL12 axis accounts for many disease indications, including tissue/nerve regeneration, cancer metastasis and inflammation. Blocking CXCR4 signaling with its antagonists may lead to moving out $CXCR4^+$ cell types from bone marrow to peripheral circulation. We have discovered a novel series of pyrimidine-based CXCR4 antagonists, a representative (i.e., **16**) of which was tolerated at a higher dose and showed better HSC-mobilizing ability at the maximal response dose relative to the approved drug **1** (AMD3100), and thus considered a potential drug candidate for PBSCT indication. Docking compound **16** into the X-ray crystal structure of CXCR4 receptor revealed that it adopted a spider-like conformation striding over both major and minor subpockets. This putative binding mode provides a new insight into CXCR4 receptor-ligand interactions for further structural modifications.

INTRODUCTION

The G protein-coupled CXC chemokine receptor 4 (CXCR4) is activated by CXCL12, also known as stromal cell-derived factor-1 or SDF-1, and is constitutively expressed in both CNS and peripheral systems.[1–5] The interaction between CXCL12 and CXCR4 can regulate the trafficking of many different cell types, such as hematopoietic stem cells (HSCs),[6] endothelial progenitor cells (EPCs)[7] and mesenchymal stem cells (MSCs).[8] Multiple functions have been found along the CXCR4/CXCL12 axis, including the promotion of angiogenesis, metastasis, tumor growth and cancer survival, neurogenesis, immunmodulation and protective/reparative effects in the lesioned tissues.[9-11] Moreover, both chemokine receptors CXCR4 and CCR5 act as co-receptors in mediating HIV-1 entry. The first-in-class CCR5 antagonist, maraviroc, was approved in 2007 as an anti-HIV drug.[12] Unfortunately, clinical observation of HIV-infected patients after maraviroc administration resulted in a X4/R5 mixed-tropic viral population with poor prognosis, suggesting that blocking both co-receptors are desirable.[13] To date, small-molecule CXCR4 antagonists **1** (AMD3100, Plerixafor, Chart 1) and AMD11070 are not being further developed for HIV-1 infection due to lack of overall clinical benefit and hepatotoxicity observed in long-term animal studies, respectively.[14–16] Another advanced CXCR4 blocker KRH-3955, displaying high potency and oral bioavailability in a HIV-1 replication model, is in early clinical development.[17]

Chart 1. Selected Small-Molecule CXCR4 Antagonists with anti-HIV-1 Activity

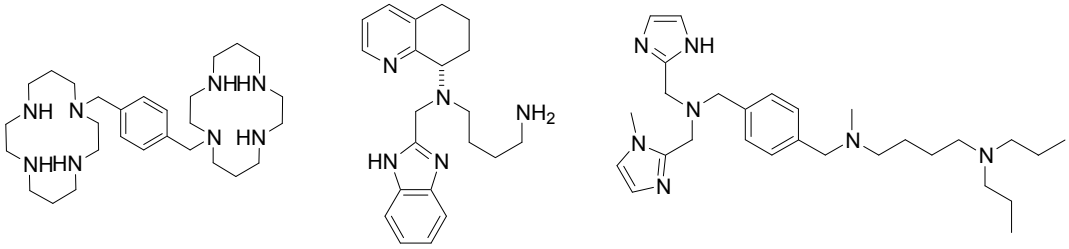

1 (AMD3100) **AMD11070** **KRH-3955**

Thus, a significant unmet medical need remains for treatment of AIDS by blocking the CXCR4-utilizing HIV strains. In addition to serving as anti-HIV agents,[18,19] increasing evidence has also strongly supported that CXCR4 specific antagonists could effectively induce functional recovery in various ischemic disease animal models associated with ischemic stroke, acute kidney injury and myocardial infarction through autologous migration of stem cells out of bone marrow into peripheral circulation.[20–25] CXCR4 may become a versatile drug target in numerous therapeutic areas, including anti-cancer metastasis,[26,27] anti-inflammation,[28–31] as well as tissue repair or nerve regeneration.[32] A specific CXCR4 antagonist **1** in combination with the granulocyte colony-stimulating factor (G-CSF; Filgrastim) has been approved by US/FDA in 2008 for use in transplantation in non-Hodgkin's lymphoma or multiple myeloma patients. It is utilized in a medical procedure called peripheral blood stem cell transplantation (PBSCT) to help cancer patients restore their immune system rapidly after chemo- or radiotherapy.[33,34] More specifically, the procedure consists of an 8-day treatment period, in which patients receive a daily dose of G-CSF for four consecutive days to stimulate stem cell

production, and beginning on day 5, a stem cell mobilizer **1** is co-injected with G-CSF daily for subsequent daily apheresis (day 5 to 8) until more than 6×10^6 $CD34^+$ cells/kg are harvested.[35,36] More importantly, it was reported that HSCs collected in this manner also showed long-term repopulating capacity, implying that the above PBSCT procedure may replace a traditional surgical operation as a favorable source for adult stem cell transplantation in the future.[37,38] Recent encouraging clinical evidence revealed that when patients with acute ischemic stroke were transplantated intra-arterially with autologous $CD34^+$ stem cells, they all showed significant improvement in functional recovery and reduction in the brain infarct volumn in the following six months after treatment.[39] Though CXCR4 antagonists are structurally diverse as seen in many historical cases,[7,22,23,40] they appear to have a preference for incorporating multiple nitrogen elements in a spider-like skeleton. This structural propensity is presumably due to mimicking highly positively charged natural ligand CXCL12, comprising a sequence of 68 amino acids rich in Lys and Arg residues.[40k] In continuation of our long-term studies on CXCR4 antagonists, herein, we wish to report that out of 600 polyamine analogues designed and experimentally realized via docking into the X-ray crystal structure of CXCR4,[41,42] a selective and potent CXCR4 antagonist **16**, named CX0714 in our in-house library, has been identified as a promising drug candidate for PBSCT and also has potential utility in many other CXCR4-mediated diseases.[43] Results are

presented as follows.

RESULTS AND DISCUSSION

The first and only marketed CXCR4 antagonist **1** is commonly considered toxic and particularly inappropriate for the chronic treatment (SI, S64 & see details in ref. 50, pp. 86–154). Therefore, we set out to identify a new generation of CXCR4-targeted compounds with better safety profiles and HSC mobilization by optimizing a series of quinazoline-core analogues previously designed in our laboratories (e.g., **2** and **3**).[23]

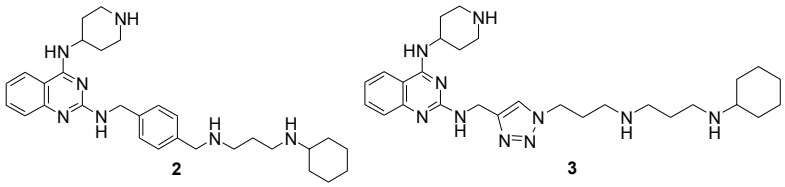

We began by simplifying the original quinazoline ring into a pyrimidine unit while maintaining the previously optimized triazole ring linker (e.g., **3**). As illustrated in Scheme 1 using compound **7** as a typical example, a general synthetic procedure was implemented to prepare an array of analogues **7**–**13**. Starting from 2,4-dichloro-6-methylpyrimidine, C4-substitution with 4-amino-1-benzyl-piperidine was established at room temperature in a chemoselective fashion to produce intermediate **4** in 62%, which in turn underwent C2-substitution with a *N*-Boc protected Linker **1** at elevated temperature (140 °C) in pentanol to afford intermediate **5** in 63%. Selective hydrogenolysis was carried out under 1 atm of hydrogen with Pd/C as catalyst to give amine **6** in 92% yield, in which *N*-Boc was subsequently deprotected under acidic

conditions (1*N* HCl) to afford desired product **7** in 95% yield as a hydrochloride salt.

Scheme 1. The Synthesis of Representative Compound 7[a]

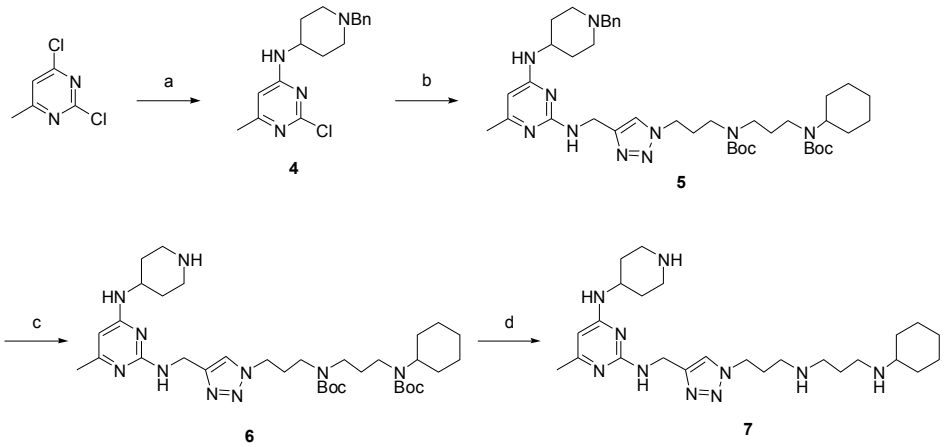

[a]Reagents and conditions: (a) 4-amino-1-Benzyl-piperidine, TEA, CH_2Cl_2, 5 °C to rt, 16 h, 62%; (b) Linker **1**, 1-pentanol, 140 °C, 5 h, 63%; (c) Pd/C (10 %), 2-propanol, 60 °C, 16 h, 92%; (d) 1*N* HCl in diethylether, CH_2Cl_2, rt, 16 h, 95%.

As listed in Table 1, when R^1 is a hydrogen or alkyl group, the corresponding compounds **7**–**10** exhibit potent binding affinities (IC_{50} = 23–61 nM) toward CXCR4 receptors, suggesting that the pyrimidine unit can replace quinazoline ring as a bioisosteric nucleus. However, as the neutral R^1 group is replaced with either a strong electron-donating (OCH_3) or electron-withdrawing (CF_3) group, a dramatic decrease in binding affinities by 10-fold is observed as demonstrated by compounds **11**–**13** (IC_{50} = 472–859 nM). In addition, an acute toxicity study revealed that all compounds in Table 1 remained toxic, showing a lower maximum tolerated dose (MTD = 10 mg/kg) than that of the positive control **1** (MTD = 15 mg/kg) following the same subcutaneous (SC) administration in mice.

Table 1. Binding Affinity and Acute Toxicity of Polyamines 7–13

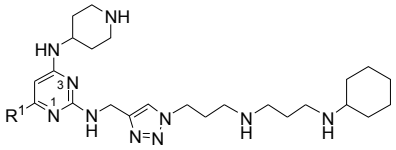

Compd	R^1	IC_{50} [nM][a]	MTD [mg/kg][b]
7	Me	23.9 ± 3.0	10
8	H	34.1 ± 3.8	10
9	Et	46.8 ± 12.9	10
10	*i*-Pr	61.1 ± 4.4	10
11	OMe	472.7 ± 136.3	10
12	Cl	708.3 ± 63.7	10
13	CF_3	859.7 ± 255.6	10
1		213.1 ± 26.0	15

[a]Determined by 50% inhibition of radioligand [^{125}I]CXCL12 binding to hCXCR4-transfected HEK293 membrane; values represent the mean ± SD of at least three independent experiments. [b]Following SC administration in C57BL/6 mice.

Further structural modifications intended for reducing acute toxicity were then attempted by elongating the side arm at C4-position while Linker **1** at C2 remained intact. In fact, the length of Linker **1** has been previously studied in the corresponding bioisosteric quinazoline series as exemplified by compound **3**.[23] Linker **1** with a [1+3+3] methylene unit was considered optimal and engrafted on the current pyrimidine series. According to Scheme 2, it could be readily prepared using propargylamine as the starting material. Propargylamine was first coupled with benzyl chloroformate to form a Cbz protected intermediate in a quantitative yield (95%), which was then reacted with 3-azido-propanol via click chemistry under catalysis with Cu(I) to generate triazole alcohol in a

regioselective manner in 83%. Triazole alcohol thus formed could further undergo mesylation to afford the corresponding mesylate (90%), which was subsequently substituted with propane-1,3-diamine followed by reductive amination with cyclohexanone and subsequent protection with Boc_2O to afford a fully *N*-protected Linker **1** in 43% yield over three steps. Finally, the Cbz protecting group was selectively

Scheme 2. Preparation of *N*-Boc Protected Linker 1[a]

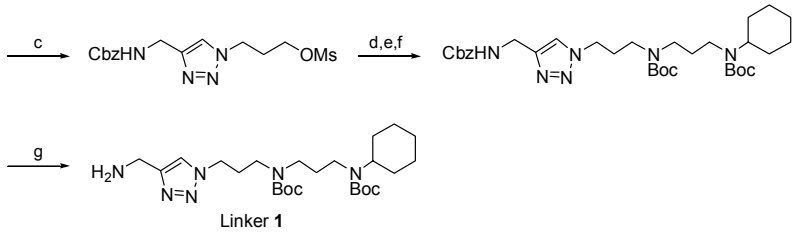

[a]Reagents and conditions: (a) benzyl chloroformate, K_2CO_3, THF/H_2O = 1/2, 5 °C to rt, 15 h, 95%; (b) 3-azido-propanol, $CuSO_4$, (+) sodium L-asorbate, K_2CO_3, EtOH/H_2O = 4/1, rt, 15 h, 83%; (c) MsCl, TEA, CH_2Cl_2, 5 °C to rt, 15 h, 90%; (d) propane-1,3-diamine, THF, 65 °C, 15 h; (e) cyclohexanone, MeOH, 60 °C, 6 h then $NaBH_4$, 5 °C, 1 h; (f) Boc_2O, CH_2Cl_2, rt, 15 h, 43% over three steps; (g) H_2, Pd/C, 2-propanol, 60 °C, 15 h, 93%.

removed via hydrogenolysis to afford the desired Linker **1** in 93% yield. As illustrated in Scheme 3 using compound **16** as a typical example, compound **7** with fixed Linker **1** at C-2 was subjected to further structural modifications via elongating the C-4 substituent by coupling with an array of amino and phosphonic acids to generate compounds **16**–**26** in 51-60% yields over three steps. Intermediate **6** was first coupled with 3-Boc-(2-ethoxy-2-oxoethyl)amino) propionic acid under catalysis with EDCI/HOBt to provide compound **14** in 71% yield, which in turn was subjected to ester hydrolysis under basic

conditions to furnish the corresponding acid **15** in quantitative yield (99%). Compound **15** was hydrolyzed under acidic conditions to remove *N*-Boc to afford the desired **16** in 95% yield as a hydrochloride salt.

Scheme 3. The Synthesis of Representative Compound 16[a]

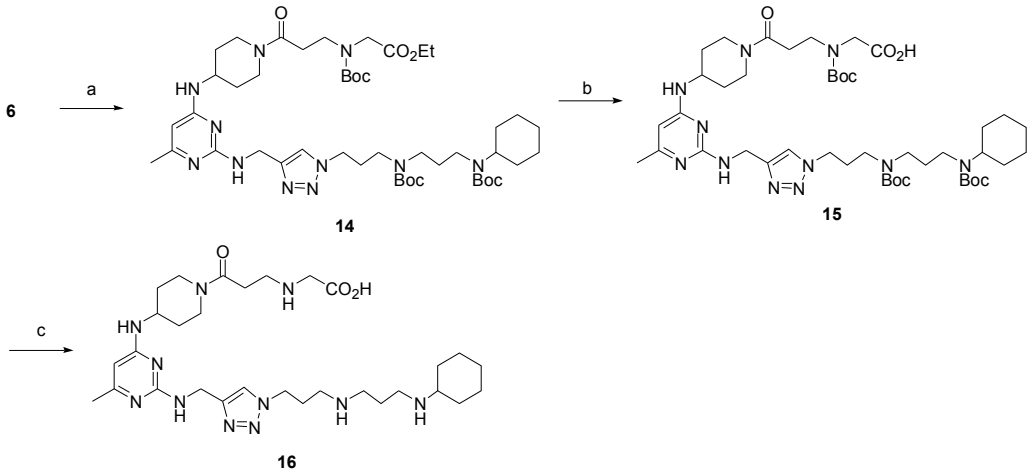

[a]Reagents and conditions: (a) 3-((*tert*-butoxycarbonyl)(2-ethoxy-2-oxoethyl)amino)propionic acid, EDCI, HOBt, CH_2Cl_2, rt, 16 h, 71%; (b) LiOH, THF/H_2O, rt, 16 h, 99%; (c) 1*N* HCl in diethylether, CH_2Cl_2, rt, 16 h, 95%.

Following a similar synthetic method starting from the same intermediate **6**, compounds **27**–**32** were synthesized as a hydrochloride salt in 50-60% yield over a two-step sequence, involving a typical S_N2 substitution followed by hydrolysis of the *N*-Boc protecting group under acidic conditions. As compiled in Table 2, both acute toxicity and structure-activity relationship (SAR) of these compounds are evaluated and elucidated as follows.

Table 2. Binding Affinity and Acute Toxicity of Polyamines 16–32

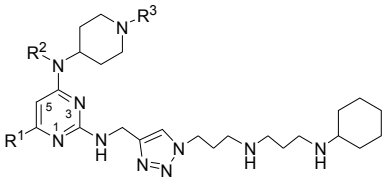

Compd	R^1	R^2	R^3	IC_{50} [nM][a]	MTD [mg/kg][b]
16	Me	H	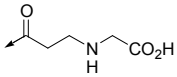	34.2 ± 6.1	75
17	Me	H	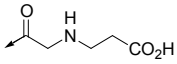	82.6 ± 12.2	100
18	Me	H	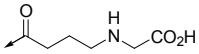	88.5 ± 16.0	75
19	Me	H	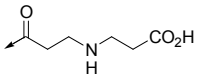	72.2 ± 13.8	50
20	Et	H	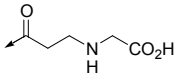	72.0 ± 19.0	50
21	H	H	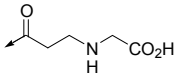	399.3 ± 73.8	100
22	Me	Me	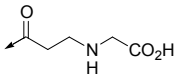	97.6 ± 9.0	50
23	Me	H	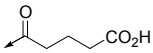	158.0 ± 19.8	50
24	Me	H	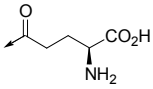	71.1 ± 9.3	50
25	Me	H	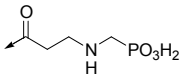	91.6 ± 9.4	100
26	Me	H	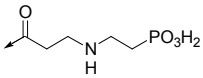	147.1 ± 33.2	75
27	Me	H		47.8 ± 9.2	10
28	Me	H		72.1 ± 21.1	20
29	Me	H		25.6 ± 8.2	20

30	Me	H	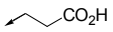	81.8 ± 4.9	75
31	Me	H	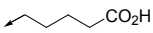	93.0 ± 3.7	75
32	Me	H		70.4 ± 19.5	100
1				213.1 ± 26.0	15

[a]Determined by 50% inhibition of radioligand [^{125}I]CXCL12 binding to hCXCR4-transfected HEK293 membrane; values represent the mean ± SD of at least three independent experiments. [b]Following SC administration in C57BL/6 mice.

In the beginning, compound **27** with an alkyl group as a R^3 side arm was first synthesized, of which binding affinity (IC_{50} = 47.8 ± 9.2 nM) and MTD (10 mg/kg) were found comparable to its parent compound **7**. When the terminal methyl moiety of **27** was changed to the cyano group, however, the MTD of the resulting compound **28** was increased by 2-fold to 20 mg/kg though binding affinity (IC_{50} = 72.1 ± 21.1 nM) was slightly decreased. This modest improvement in MTD prompted us to modify the R^3 spacer with more polar terminal groups. Changing the cyano to an amide group resulted in compound **29** with little enhancement in potency (IC_{50} = 25.6 ± 8.2 nM), but acute toxicity was retained (MTD = 20 mg/kg). When the amide group was further changed to the carboxylic functionality, the resulting compounds **30**–**32** (IC_{50} = 70.4–93.0 nM, MTD = 75–100 mg/kg) showed a sharp increase in MTD though their binding activities decreased by 3-fold relative to parent **7** (IC_{50} = 23.9 ± 3.0 nM, MTD = 10 mg/kg), suggesting that a polar carboxylic group at the terminus of the C-4 substituent could significantly reduce acute toxicity. As such, this functionality is kept constant while

other portions of the pharmacophore are varied in further structural modifications. In the meantime, to make the C-4 linker synthetically more variable and practical, two new structural elements including a carbonyl moiety and nitrogen were appropriately incorporated into the linker. As a result, compounds **16–19** (IC_{50} = 34.2–88.5 nM, MTD = 50–100 mg/kg) were then prepared. As demonstrated with **16** (IC_{50} = 34.2 ± 6.1 nM, MTD = 75 mg/kg), the C-4 linker containing [2+1] methylene units appeared optimal in length in terms of potency and acute toxicity. Keeping it as a fixed theme, we slightly altered R^1 and R^2 groups to afford structurally closely related analogues **20–24** (IC_{50} = 71.1–399.3 nM, 50–100 mg/kg). Unfortunately, these modifications led to losing binding affinities by 2- to 10-fold relative to **16** though their MTD remained at a satisfactory level. Replacing the terminal carboxylic group with its equivalent, phosphonic acid, was also explored; however, the resulting compounds **25** (IC_{50} = 91.6 ± 9.4 nM) and **26** (IC_{50} = 147.1 ± 33.2 nM) showed no improvement in binding affinities though their MTD still maintained at a high level (50–100 mg/kg). The higher MTD seen in this novel series of compounds than bicyclam **1** is presumably due to the presence of the terminal carboxylic or phosphonic acid, allowing to increase protein binding and decrease distribution (e.g., **16**, 60~75% vs **1**, 33~50% in rats). However, the underlying cause remains to be determined. Compound **16** (IC_{50} = 34.2 ± 6.1 nM; MTD = 75 mg/kg, SC) possessing a much stronger binding affinity and higher MTD than the

marketed drug **1** (IC_{50} = 213.1 ± 26.0 nM; MTD = 15 mg/kg, SC) was considered a potential drug candidate and elected for various preclinical evaluations as shown below.

To examine compound **16**'s specificity among chemokine family, it was extensively screened against a panel of chemokine receptors in both CCR and CXCR types. As listed in Table 3, compound **16** exhibited no cross-activity up to 10 μM in cAMP functional assay toward all tested receptors (-11~0.5% inhibition) except CXCR4 (73.4% inhibition), indicating that it is a highly selective CXCR4 antagonist (see SI, S10–S21).

Table 3. Selectivity of Compound 16 against Related Chemokine Receptors

Assay Target	CCR1	CCR5	CCR6	CCR7	CCR10	XCR1
Efficacy [%][a]	-1.2	0.5	-2.2	-4.2	0.5	-2.8
Assay Target	CXCR1	CXCR2	CXCR3	CXCR4	CXCR5	CXCR6
Efficacy [%][a]	0.3	0.5	-7.6	73.4	-11	-3.9

[a]Percentage inhibition was determined in GPCR cAMP assay at a concentration of 10 μM; very weak inhibition (0.5~-11%) was observed for all tested chemokine receptors except CXCR4 (73.4%).

Subsequently, the chemotaxis assay was conducted to evaluate compound **16**'s role in cellular migration of $CXCR4^+$ cells. As indicated in Figure 1, CXCL12-induced movement of CCRF-CEM cells, a human cell line highly expressed with CXCR4, was efficiently blocked at a very low concentration (EC_{50} = 13.7 ± 3.8 nM). Compound **16** was also subjected to the cytotoxicity assay against Detroit 551 (human normal skin

fibroblast cells) with a CC_{50} value of more than 100 μM. Taken together, above *in vitro* studies suggest that compound **16** is a highly selective CXCR4 antagonist and tolerated up to high doses in mice.

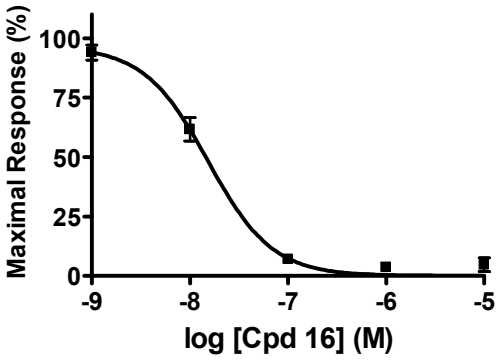

Figure 1. CXCL12-induced chemotaxis assay was conducted for compound **16**. Data were collected from three independent experiments and represent the mean ± SD.

For comparison purposes, pharmacokinetic studies on both control **1** and **16** were carried out simultaneously prior to *in vivo* studies, results of which were summarized in Table 4. Accordingly, compound **16**'s blood exposure (AUC = 13515 ng/mL· h) and C_{max} (16400 ng/mL) are almost 2 times as high as drug **1** (AUC = 7152 ng/mL· h; C_{max} = 6200 ng/mL).

Table 4. Pharmacokinetic Studies of Control 1 and Compound 16[a]

Compd	route	dose (mg/kg)	C_{max} (ng/mL)	$T_{1/2}$ (h)	$AUC_{(0\text{-}4h)}$ (ng/mL· h)
1	SC	6	6200 ± 394	1.4 ± 0.6	7152 ± 135
16	SC	6	16400 ± 2858	0.5 ± 0.1	13515 ± 1618

[a]Values indicate mean ± SD (n = 3) following SC in C57BL/6 mice.

Meanwhile, from the mechanistic point of view, CXCR4 antagonists are supposed to be eliminated timely when stem cells circulating in peripheral blood are collected. Thus,

compound **16** with $T_{1/2}$ = 30 min, presumably due to phase II metabolism by kidney, apparently meets with this pharmacokinetic requirement for PBSCT indication. To determine its maximal response dose, compound **16** was administered subcutaneously at an escalating dose of 1, 6, 20, 35 and 50 mg/kg, respectively, in 8- to 10-week-old C57BL/6 male mice. As a result, a dose dependent curve of the number of $CXCR4^+$ stem cells was observed via the flow cytometry analysis as illustrated in Figure 2.

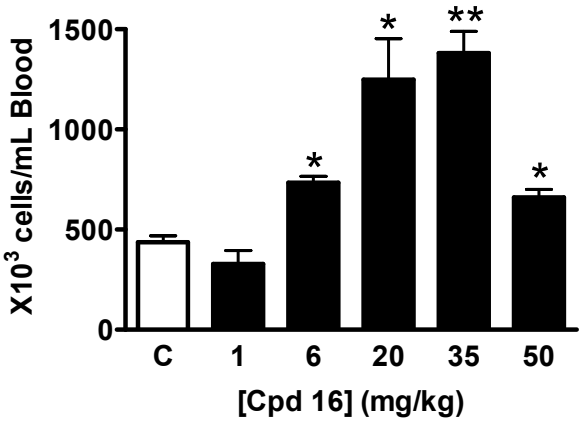

Figure 2. $CXCR4^+$ cells were analyzed by flow cytometry. The blood samples containing mobilized $CXCR4^+$ stem cells were collected from C57BL/6 mice and measured by flow cytometry at a time point of 2 h after SC injection with indicated concentrations of compound **16**. Data represent the mean ± SEM (n = 3 per group). Statistical analysis was performed by *t* test: $*p < 0.05$ and $**p < 0.01$ between control and the indicated test group.

A 3-fold ($p < 0.01$) increase in $CXCR4^+$ stem cells was observed at a dose of 35 mg/kg, tentatively assigned as a maximal response dose, as compared to vehicle,. Since its minimal effect dose (MED) occurred at 6 mg/kg, thus, the therapeutic window was determined as MTD/MED = 12.5. More than the maximal response dose resulted in a significant decrease in the number of $CXCR4^+$ stem cells as observed at a dose of 50

mg/kg ($p < 0.05$). We are particularly interested in $CD34^+$ and $CD133^+$ as well as $VEGFR2^+$ and $VEGFR2^+Sca\text{-}1^+$ cell types; the former ($CD34^+$ and $CD133^+$) are widely recognized as biomarkers for HSCs[44,45] and the latter are for EPCs.[46,47] Thus, double staining experiments (e.g., $CXCR4^+/CD34^+$) were further performed and results were analyzed as follows. A maximal response dose of positive control **1** (6 mg/kg) and test compound **16** (35 mg/kg) was given via SC injection, respectively, to evaluate their ceiling effects on moving out HSCs and EPCs stem cells.[48] As displayed in Figures 3 (A), (B), (C) and (D), treatment with compound **16** alone did exhibit greater ability than marketed drug **1** as well as vehicle by about 2- and 7-fold, respectively, to move out HSCs and EPCs into the peripheral circulation. Following the clinical protocol of positive control **1**, however, compound **16** in combination with G-CSF was further examined to evaluate its combination effects on moving out HSCs. Since the experiment is critical for determining whether **16** is qualified as a drug candidate for PBSCT, instead of the primary assay using flow cytometry, a more accurate but time-consuming CFU assay was then conducted to analyze HSC counts between dosing with **1**+GCSF and **16**+GCSF.

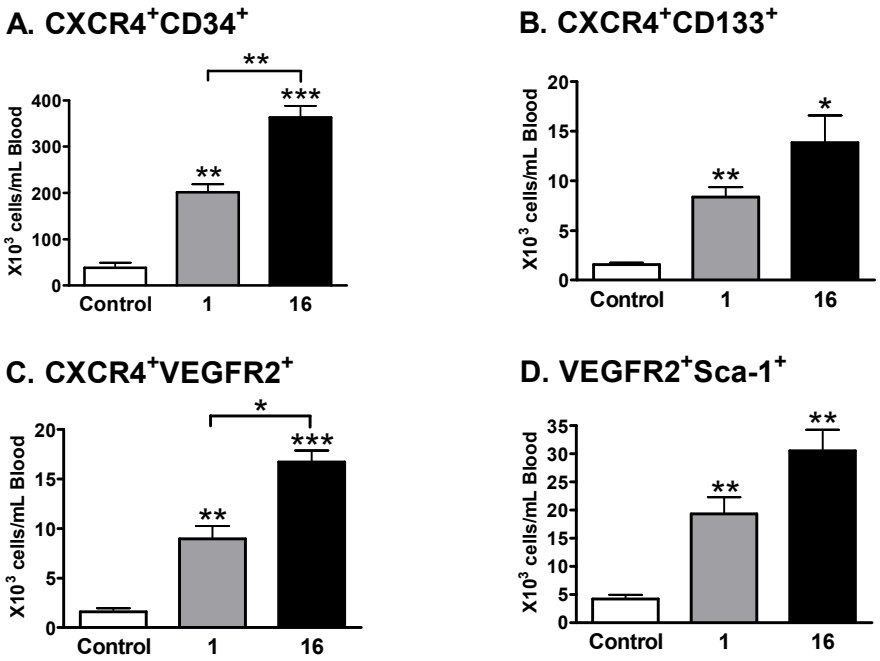

Figure 3. Double staining analysis by flow cytometry. (A) $CXCR4^+CD34^+$ cells, (B) $CXCR4^+CD133^+$ cells, (C) $CXCR4^+VEGFR2^+$ cells, and (D) $VEGFR2^+Sca\text{-}1^+$ cells. The blood samples were collected from C57BL/6 mice and measured by flow cytometry at a time point of 2 h after SC injection of compound **1** (6 mg/kg) or **16** (35 mg/kg) at the maximal response dose. Data represent the mean ± SEM (n = 3 per group). Statistical analysis was performed by *t* test: $*p < 0.05$, $**p < 0.01$, and $***p < 0.001$ between control and the indicated test group.

Peripheral blood mononuclear cells (PBMCs) were first isolated from blood samples and incubated for 10–14 days until CFU-GM (colony-forming unit-granulocyte/monocyte) colonies could be clearly formed and unambiguously counted under an inverted microscope. In general, the aggregate equal to or more than 50 cells is recorded as a colony. As seen in Figure 4, the number of CFU-GM colonies provided by **16**+GCSF was significantly increased by 1.6-fold relative to **1**+GCSF, interestingly which was in good agreement with the $CD34^+$ and $CD133^+$ cell population ratio (1.7:1) obtained by flow cytometry as illustrated in Figures 3A and 3B. Also emphasized is the fact that the

number of HSCs, as demonstrated by CFU-GM colonies, was dramatically increased by roughly 5.3-fold in the combination regimen compared to control using G-CSF alone.

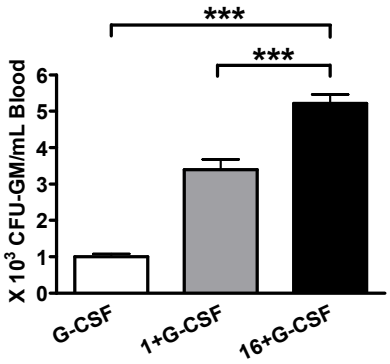

Figure 4. *In Vivo* efficacy comparison in colony-forming assay. C57BL/6 male mice were treated with G-CSF (100 μg/kg) daily for 4 consecutive days by SC injection. On day 5, G-CSF (100 μg/kg) in combination with **1** (6 mg/kg) or **16** (35 mg/kg) was given, respectively. The heparinized blood samples containing mobilized stem cells were collected 2 h after SC administration, and then peripheral blood mononuclear cells (PBMCs) were isolated and cultured for CFU-GM colony-forming assay. Data represent the mean ± SEM with 8-12 mice per group. Statistical analysis was performed by *t* test: ***$p < 0.001$ between control (G-CSF alone) and the indicated test group.

Compound **16** was also subjected to 68 off-target standard assays (SI, S2–S9). Accordingly, besides calcium channel N-type and muscarinic M2 sodium channel with 73% and 70% inhibition at 10 μM, respectively, compound **16** showed low binding and inhibitory activity toward other 66 off-targets (<50% inhibition at 10 μM). In addition, no hERG liability was observed for compound **16** at a concentration up to 100 μM in the patch-clamp assay (SI, S25–S35). Effects of compound **16** on 6 human liver microsomal CYP enzymes, including 1A2, 2C9, 2C19, 2D6, 2E1 and 3A4, were also investigated and results showed that IC_{50} values against above CYP enzymes were all greater than 100 μM, implying that drug-drug interactions caused by co-administration with

compound **16** are not likely to be a major issue. In addition to moving out HSCs and EPCs mentioned above, many CXCR4^{+} mature immune cells such as white blood cells (WBCs), also referred to as leukocytes, could be released by CXCR4 antagonists **1** and **16** as shown in Figure 5A.

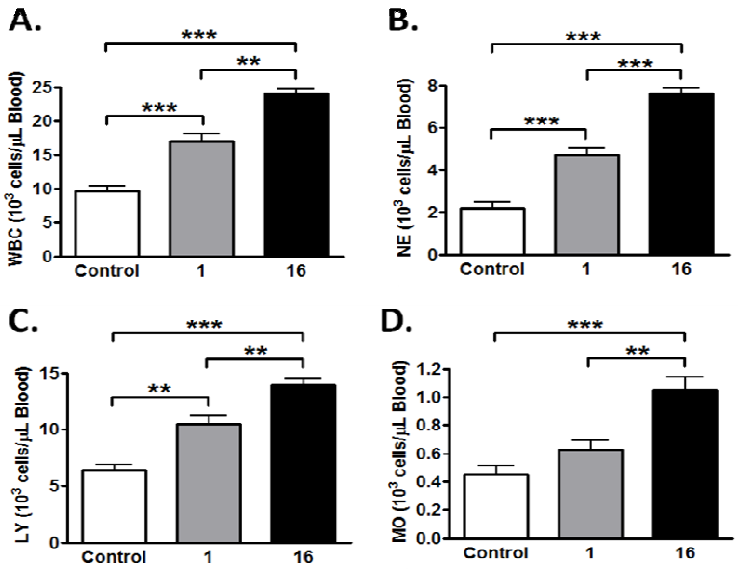

Figure 5. *In Vivo* efficacy comparison in WBC mobilization. The blood samples containing mobilized white blood cells were collected from C57BL/6 mice and analyzed for (A) total white blood cells, (B) neutrophils, (C) lymphocytes, and (D) monocytes at a time point of 2 h after SC injection with compound **1** (6 mg/kg) or **16** (35 mg/kg). Data represent the mean ± SEM (n = 5 per group). Statistical analysis was performed by *t* test: $*p < 0.05$, $**p < 0.01$, and $***p < 0.001$ between the indicated test group.

In general, WBCs are composed of neutrophils, eosinophils, basophils, lymphocytes and monocytes.[49] As seen in Figures 5B, 5C and 5D, compound **16** can mobilize out neutrophils, lymphocytes and monocytes, which are mainly responsible for anti-infection, activating immunity and engulfing antigens in the living system, in cell counts higher than drug **1** by 30~50%, and more than control by 2- to 4-fold, again verifying that it is a versatile CXCR4-targeted agent.

To further support compound **16** as a suitable drug candidate, its non-GLP 14-day repeated dose toxicology study (SD rats, 50 mg/kg/day, SC) has been carried out, results of which revealed that all major organs, including liver, kidney, lung, heart, etc, are normal in size, weight and color as compared to those in vehicle. As well, blood sample analysis also showed that no significance difference was observed in both hematological and biochemical data between vehicle and experimental rats (SI, S65–S67). Since structurally compound **16** is a polyamine and highly suspected to be metabolized by kidney as seen with compound **1**,[50] an acute histology study on kidney was also performed. Consequently, no specific histological difference was found in renal tissue between the control and experimental groups at a dose up to 100 mg/kg as analyzed by photomicrographs illustrated in Figures S1 and S2 (SI, S68–S69).

To better understand the SAR of this newly developed series, computational docking studies were extensively undertaken during the course of development. As typified by Figure 6, molecular docking of **16** to the X-ray structure of CXCR4 (PDB ID: 4RWS) displayed that secondary amino and carboxylic groups of **16** could form hydrogen bonding/polar interactions with Asn33, Asn37, Asp97, His203, Gly207 and Tyr256 (cyan) constituting the major subpocket, and the terminal cyclohexyl ring was anchored

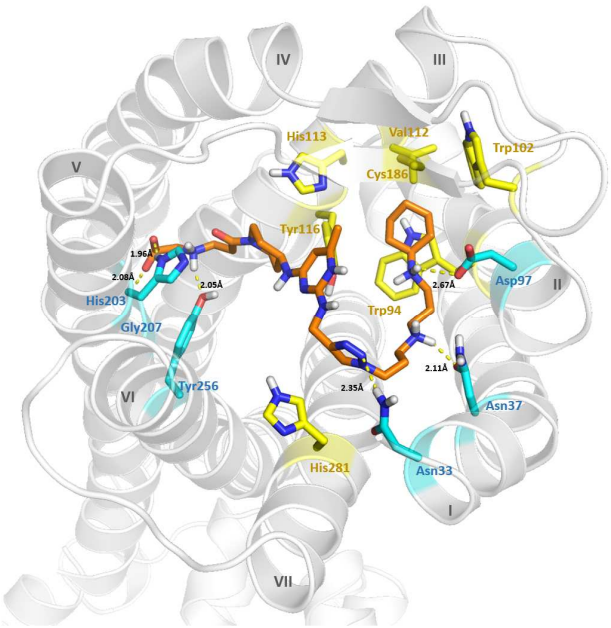

Figure 6. Docking compound **16** (Orange) to the CXCR4 crystal structure (PDB ID: 4RWS) after 20 ns of MD simulations.

at the minor subpocket surrounded by a series of hydrophobic residues Trp94, Trp102, Val112, His113, Tyr116 and Cys186 (yellow). This putative binding mode, crossing both major and minor binding pockets, could be further highlighted via superimposing the above simulating complex structure on both X-ray co-crystal structures IT1t/3ODU and CVX15/3OE0. As illustrated in Figure 7, it clearly demonstrates that different from the cyclic peptide CVX15 (pink) interacting with the major subpocket and small molecule IT1t (green) with the minor subpocket, compound **16** (orange) assumes a stretching-out conformation to occupy both major and minor subpockets simultaneously.[41] This spider-like putative binding mode seems to interact favorably with the open and negatively charged CXCR4 receptor, and provides a new insight into CXCR4 receptor-ligand interactions, whereby more effective CXCR4 antagonists with improved oral

bioavailability might be developed in the future.

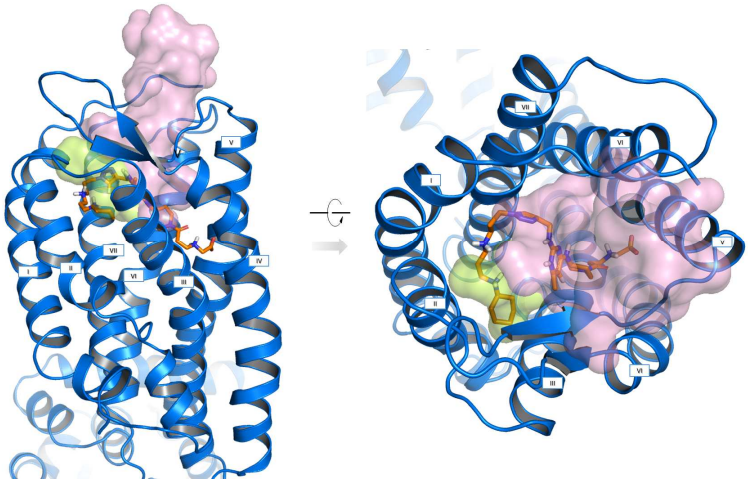

Figure 7. Compound **16** (orange) is assumed to occupy both major and minor subpockets displayed with a pink (CVX15) and green (IT1t) surface field.

CONCLUSION

Though currently autologous adult stem cell transplantation is the only therapeutic utility for CXCR4-targeted agents (e.g., **1**), CXCR4 might become an important drug target in light of its versatile mechanistic pathways.[9] We have discovered a novel series of pyrimidine-based CXCR4 antagonists, the representative (i.e., **16**) of which apparently exhibited a higher MTD dose and better HSC/EPC-mobilizing ability at the maximal response dose than drug **1** in mice following SC administration, suggesting that compound **16** could serve as a promising drug candidate for PBSCT and other disease indications. In addition, inspired with the putative binding mode of this novel series of compounds, further structural modifications will be carried out to generate a second generation of CXCR4 antagonists with potential enhancement in safety profiles and oral

bioavailability.

EXPERIMENTAL SECTION

General. Unless otherwise stated, all materials used were commercially available and used as supplied. Reactions requiring anhydrous conditions were performed in flame-dried glassware and cooled under an argon or nitrogen atmosphere. Unless otherwise stated, reactions were carried out under argon or nitrogen and monitored by analytical thin layer chromatography performed on glass-backed plates (5 × 10 cm) precoated with silica gel 60 F254 as supplied by Merck. Visualization of the resulting chromatograms was performed by looking under an ultraviolet lamp (λ = 254 nm) followed by dipping in an ethanol solution of vanillin (5% w/v) containing sulfuric acid (3% v/v) or phosphomolybdic acid (2.5% w/v) and charring with a heat gun. Flash chromatography was used routinely for purification and separation of product mixtures using silica gel 60 of 230−400 mesh size as supplied by Merck. Eluent systems are given in volume/volume concentrations. Melting points were determined using a KRUSS KIP1N melting point meter. ^{1}H and ^{13}C NMR spectra were recorded on a Varian Mercury-300 (300 MHz) and a Varian Mercury-400 (400 MHz). Chloroform-d, methanol-d4 or deuterium oxide-d2 was used as the solvent and TMS (δ 0.00 ppm) as an internal standard. Chemical shift values are reported in ppm relative to the TMS in delta (δ) units. Multiplicities are recorded as s (singlet), br s (broad singlet), d (doublet), t (triplet), q

(quartet), dd (doublet of doublets), dt (doublet of triplets), and m (multiplet). Coupling constants (*J*) are expressed in hertz. Electrospray mass spectra (ESMS) were recorded as *m/z* values using an Agilent 1100 MSD mass spectrometer. All test compounds displayed more than 95% purity as determined by an Agilent 1100 series HPLC system using a C18 column (Thermo Golden, 4.6 mm × 250 mm). The gradient system for HPLC separation was composed of MeOH (mobile phase A) and H_2O solution containing 0.1% trifluoro-acetic acid (mobile phase B). The starting flow rate was 0.5 mL/min and the injection volume was 10 μL. During first 2 min the percentage of phase A was 10%. At 6 min, the percentage of phase A was increased to 50%. At 16 min, the percentage of phase A was increased to 90% over 9 min. The system was operated at 25 ^{o}C. Peaks were detected at 254 nm. IUPAC nomenclature of compounds was determined with ACD/Name Pro software. All novel compounds reported here were screened for PAINS using KNIME: PAINS-Indigo (module) software, and results showed that no PAINS liability was detected for them.[51]

(1-Benzyl-piperidin-4-yl)-(2-chloro-6-methyl-pyrimidin-4-yl)-amine (4). A solution of 2,4-dichloro-6-methylpyrimidine (1.00 g, 6.1 mmole), 1-Benzyl-piperidin-4-ylamine (1.20 g, 6.3 mmole), and TEA (0.92 g, 9.1 mmole) in THF (72 mL) under an atmosphere of nitrogen was stirred at 25 ^{o}C for 15 h and then quenched with aqueous NH_4Cl. The resulting mixture was extracted with ethyl acetate. The combined organic extracts were

washed with brine, dried over anhydrous sodium sulfate, filtered, and concentrated. The residue thus obtained was purified by flash chromatography on silica gel with *n*-hexane/ethyl acetate (1:1) to give compound **4** (1.20 g, 62%) as sticky oil. ^{1}H NMR (300 MHz, $CDCl_3$) δ 7.35−7.21 (m, 5H), 6.05 (s, 1H), 3.62 (m, 1H), 3.52 (s, 2H), 2.82 (m, 2H), 2.32 (s, 3H), 2.19 (m, 2H), 1.98 (m, 2H), 1.55 (m, 2H). ESMS *m/z*: 317.5 (M+1).

[3-(4-{[4-(1-Benzyl-piperidin-4-ylamino)-6-methyl-pyrimidin-2-ylamino]-methyl}-[1,2,3]triazol-1-yl)-propyl]-[3-(tert-butoxycarbonyl-cyclohexyl-amino)-propyl]-carbamic acid tert-butyl ester (5). A solution of compound **4** (1.01 g, 3.19 mmole) and Linker **1** (1.74 g, 3.52 mmole) in 1-pentanol (25 mL) was heated at 150 ^{o}C for 15 h and then concentrated. The residue thus obtained was purified by flash chromatography on silica gel with MeOH/DCM (1:32) to afford compound **5** (1.55 g, 63%) as sticky oil. ^{1}H NMR (400 MHz, $CDCl_3$) δ 7.61 (s, 1H), 7.34−7.21 (m, 5H), 5.59 (s, 1H), 4.68 (m, 2H), 4.30 (t, J = 7.2 Hz, 2H), 3.87 (m, 1H), 3.52 (s, 2H), 3.26−2.98 (m, 6H), 2.84 (m, 2H), 2.20 (s, 3H), 2.19−2.04 (m, 6H), 1.98 (m, 2H), 1.80−1.46 (m, 7H), 1.44 (s, 18H), 1.40−1.22 (m, 5H), 1.05 (m, 1H). ESMS *m/z*: 775.6 (M+1).

[3-(tert-Butoxycarbonyl-cyclohexyl-amino)-propyl]-[3-(4-{[4-methyl-6-(piperidin-4-ylamino)-pyrimidin-2-ylamino]-methyl}-[1,2,3]triazol-1-yl)-propyl]-carbamic acid tert-butyl ester (6). A solution of **5** (1.50 g, 1.94 mmole) and 10% Pd/C (0.15 g) in 2-propanol (30 mL) was stirred under H_2 (1 atm) at 60 ^{o}C for 15 h. The resulting mixture

was filtered and the filtrate was concentrated to give **6** (1.22 g, 92%) as a white solid: mp 182.3-182.7 ^{o}C. ^{1}H NMR (400 MHz, $CDCl_3$) δ 7.82 (s, 1H), 6.20 (s, 1H), 4.70 (s, 2H), 4.41−4.30 (m, 3H), 3.59 (m, 2H), 3.32−2.98 (m, 8H), 2.25 (s, 3H), 2.22−2.00 (m, 6H), 1.82−1.59 (m, 7H), 1.44 (s, 18H), 1.40−1.20 (m, 5H), 1.05 (m, 1H). ESMS *m/z*: 685.5 (M+1).

N2-{1-[3-(3-Cyclohexylamino-propylamino)-propyl]-1H-[1,2,3]triazol-4-ylmethyl}-6-methyl-N4-piperidin-4-yl-pyrimidine-2,4-diamine hydrochloride salt (7). A solution of 1*N* HCl/ether (5.13 mL, 5.13 mmole) was added to the solution of **6** (344 mg, 0.51 mmole) in dichloromethane (6.88 mL). The mixture was stirred at 25 ^{o}C for 15 h and concentrated to afford **7** (300 mg, 95%). ^{1}H NMR (300 MHz, D_2O) δ 8.02 (s, 1H), 5.93 (s, 1H), 4.75 (s, 2H), 4.56 (t, *J* = 6.9 Hz, 2H), 4.17 (m, 1H), 3.46 (m, 2H), 3.21−3.04 (m, 8H), 2.33 (m, 2H), 2.25 (s, 3H), 2.16−1.99 (m, 6H), 1.87−1.62 (m, 5H), 1.40−1.17 (m, 6H). ^{13}C NMR (100 MHz, D_2O) δ 162.54, 153.85, 152.27, 145.46, 123.69, 96.56, 57.40, 47.38, 45.27, 44.71, 44.58, 42.60, 41.14, 36.14, 28.73, 27.18, 26.12, 24.36, 23.78, 22.79, 17.66. ESMS *m/z*: 485.5 (M+1). HPLC purity = 96.92%, tR = 13.04 min.

N2-{1-[3-(3-Cyclohexylamino-propylamino)-propyl]-1H-[1,2,3]triazol-4-ylmethyl}-N4-piperidin-4-yl-pyrimidine-2,4-diamine hydrochloride salt (8). Following a similar synthetic procedure for compound **7**, products **8**−**13** were prepared in a sequence of four steps using various 2,4-dichloropyrimidine derivatives as starting material.

Starting from 2,4-dichloropyrimidine (500 mg, 3.36 mmole), compound **8** (641 mg) was obtained in 31% yield over four steps. ^{1}H NMR (300 MHz, D_2O) δ 8.06 (s, 1H), 7.56 (d, *J* = 7.2 Hz, 1H), 6.11 (d, *J* = 7.2 Hz, 1H), 4.75 (s, 2H), 4.56 (t, *J* = 6.9 Hz, 2H), 4.19 (m, 1H), 3.47 (m, 2H), 3.22−3.06 (m, 8H), 2.33 (m, 2H), 2.18−1.99 (m, 6H), 1.85−1.59 (m, 5H), 1.40−1.17 (m, 6H). ^{13}C NMR (75 MHz, D_2O) δ 162.14, 153.36, 145.28, 140.34, 123.73, 98.20, 57.38, 47.39, 45.33, 44.71, 44.58, 42.58, 41.15, 36.11, 28.72, 27.04, 26.14, 24.37, 23.79, 22.80. ESMS *m/z*: 471.4 (M+1). HPLC purity = 97.42%, tR = 12.71 min.

N2-{1-[3-(3-Cyclohexylamino-propylamino)-propyl]-1H-[1,2,3]triazol-4-ylmethyl}-6-ethyl-N4-piperidin-4-yl-pyrimidine-2,4-diamine hydrochloride salt (9). Starting from 2,4-dichloro-6-ethyl pyrimidine (503 mg, 2.84 mmole), compound **9** (513 mg) was obtained in 28% yield over four steps. ^{1}H NMR (300 MHz, D_2O) δ 8.04 (s, 1H), 5.96 (s, 1H), 4.77 (s, 2H), 4.57 (t, *J* = 6.8 Hz, 2H), 4.19 (m, 1H), 3.46 (m, 2H), 3.22−3.08 (m, 8H), 2.56 (q, *J* = 7.5 Hz, 2H), 2.36 (m, 2H), 2.18−2.00 (m, 6H), 1.88−1.60 (m, 5H), 1.40−1.17 (m, 9H). ^{13}C NMR (100 MHz, D_2O) δ 162.71, 157.40, 153.92, 145.49, 123.67, 95.12, 57.39, 47.38, 45.32, 44.72, 44.59, 42.60, 41.15, 36.18, 28.73, 27.18, 26.14, 25.10, 24.38, 23.79, 22.81, 10.84. ESMS *m/z*: 499.5 (M+1). HPLC purity = 97.92%, tR = 13.17 min.

N2-{1-[3-(3-Cyclohexylamino-propylamino)-propyl]-1H-[1,2,3]triazol-4-ylmethyl}-

6-isopropyl-N4-piperidin-4-yl-pyrimidine-2,4-diamine hydrochloride salt (10). Starting from 2,4-dichloro-6-isopropyl pyrimidine (505 mg, 2.64 mmole), compound **10** (453 mg) was obtained in 26% yield over four steps. ^{1}H NMR (400 MHz, D_2O) δ 8.02 (s, 1H), 5.94 (s, 1H), 4.75 (s, 2H), 4.55 (t, *J* = 6.8 Hz, 2H), 4.18 (m, 1H), 3.46 (m, 2H), 3.21−3.06 (m, 8H), 2.79 (m, 1H), 2.34 (m, 2H), 2.18−1.99 (m, 6H), 1.88−1.62 (m, 5H), 1.40−1.17 (m, 12H). ^{13}C NMR (100 MHz, D_2O) δ 162.84, 161.28, 154.05, 145.65, 123.55, 93.73, 57.39, 47.29, 45.32, 44.72, 44.56, 42.60, 41.12, 36.22, 31.15, 28.73, 27.17, 26.14, 24.36, 23.78, 22.79, 19.68. ESMS *m/z*: 513.5 (M+1). HPLC purity = 98.68%, tR = 13.52 min.

N2-{1-[3-(3-Cyclohexylamino-propylamino)-propyl]-1H-[1,2,3]triazol-4-ylmethyl}-6-methoxy-N4-piperidin-4-yl-pyrimidine-2,4-diamine trifluoroacetic acid salt (11). Starting from 2,4,6-trichloro pyrimidine (501 mg, 2.73 mmole), compound **11** (470 mg) was obtained in 18% yield over five steps. ^{1}H NMR (400 MHz, D_2O) δ 7.89 (s, 1H), 5.25 (s, 1H), 4.53 (s, 2H), 4.36 (t, *J* = 6.4 Hz, 2H), 3.87 (m, 1H), 3.69 (s, 3H), 3.24 (m, 2H), 2.98−2.81 (m, 8H), 2.12 (m, 2H), 1.83−1.76 (m, 6H), 1.63−1.40 (m, 5H), 1.19−0.86 (m, 6H). ^{13}C NMR (100 MHz, D_2O) δ 164.36, 162.40 (q, *J* = 36.1 Hz, $CF_3\underline{C}O_2H$), 153.35, 144.87, 143.56, 124.40, 116.24 (q, *J* = 289.8 Hz, $\underline{C}F_3CO_2H$), 75.44, 57.59, 56.92, 48.03, 45.88, 44.78, 44.71, 42.71, 41.25, 35.83, 28.86, 27.54, 26.04, 24.50, 23.93, 22.92. ESMS *m/z*: 501.5 (M+1). HPLC purity = 99.10%, tR = 13.18 min.

6-Chloro-N2-{1-[3-(3-cyclohexylamino-propylamino)-propyl]-1H-[1,2,3]triazol-4-ylmethyl}-N4-piperidin-4-yl-pyrimidine-2,4-diamine hydrochloride salt (12). Starting from 2,4,6-trichloro pyrimidine (503 mg, 2.74 mmole), compound **12** (536 mg) was obtained in 30% yield over four steps. ^{1}H NMR (300 MHz, D_2O) δ 8.02 (s, 1H), 6.22 (s, 1H), 4.75 (s, 2H), 4.55 (t, *J* = 6.6 Hz, 2H), 4.17 (m, 1H), 3.45 (m, 2H), 3.21−3.04 (m, 8H), 2.32 (m, 2H), 2.16−2.00 (m, 6H), 1.90−1.60 (m, 5H), 1.41−1.13 (m, 6H). ^{13}C NMR (75 MHz, D_2O) δ 161.83, 153.92, 144.69, 143.63, 124.00, 97.36, 57.38, 47.58, 45.79, 44.67, 44.58, 42.51, 41.15, 36.26, 28.71, 27.01, 26.05, 24.35, 23.77, 22.80. ESMS *m/z*: 505.4 (M+1). HPLC purity = 97.20%, tR = 13.16 min.

N2-{1-[3-(3-Cyclohexylamino-propylamino)-propyl]-1H-[1,2,3]triazol-4-ylmethyl}-N4-piperidin-4-yl-6-trifluoromethyl-pyrimidine-2,4-diamine hydrochloride salt (13). Starting from 2,4-dichloro-6-trifluoromethyl pyrimidine (501 mg, 2.31 mmole), compound **3** (443 mg) was obtained in 28% yield over four steps. ^{1}H NMR (300 MHz, D_2O) δ 8.02 (s, 1H), 6.53 (s, 1H), 4.79 (s, 2H), 4.56 (t, *J* = 6.6 Hz, 2H), 4.25 (m, 1H), 3.49 (m, 2H), 3.21−3.04 (m, 8H), 2.34 (m, 2H), 2.18−2.00 (m, 6H), 1.86−1.60 (m, 5H), 1.40−1.17 (m, 6H). ^{13}C NMR (75 MHz, D_2O) δ 161.40, 153.95, 144.88, 139.86 (q, *J* = 31.5 Hz), 123.77, 118.51 (q, *J* = 271.5 Hz), 97.63 (q, *J* = 4.6 Hz), 57.38, 47.41, 46.02, 44.71, 44.58, 42.51, 41.15, 36.49, 28.72, 26.77, 26.13, 24.35, 23.77, 22.80. ESMS *m/z*: 539.5 (M+1). HPLC purity = 96.61%, tR = 13.90 min.

(tert-Butoxycarbonyl-{3-[4-(2-{[1-(3-{tert-butoxycarbonyl-[3-(tert-butoxycarbonyl-cyclohexyl-amino)-propyl]-amino}-propyl)-1H-[1,2,3]triazol-4-ylmethyl]-amino}-6-methyl-pyrimidin-4-ylamino)-piperidin-1-yl]-3-oxo-propyl}-amino)-acetic acid ethyl ester (14). To a magnetically stirred solution of 3-((tert-butoxycarbonyl)(2-ethoxy-2-oxoethyl)amino)propionic acid (395 mg, 1.44 mmole) in dichloromethane (50 mL) under an atmosphere of nitrogen was added EDCI (210 mg, 1.10 mmole) and HOBt (165 mg, 1.22 mmole) at 25 ^{o}C. After the mixture was stirred at 25 ^{o}C for 1 h, a solution of **6** (490 mg, 0.72 mmole) in dichloromethane (2 mL) was added to the mixture in one potion. The reaction mixture was stirred for another 6 h and then poured into water. The resulting mixture was extracted with dichloromethane. The combined organic extracts were washed with brine, dried over anhydrous sodium sulfate, filtered, and concentrated. The residue thus obtained was purified by flash chromatography on silica gel with MeOH/DCM (1:19) to give **14** (480 mg, 71%) as sticky oil. ^{1}H NMR (400 MHz, $CDCl_3$) δ 7.62 (s, 1H), 5.63 (s, 1H), 4.65 (s, 2H), 4.41 (m, 1H), 4.29 (t, J = 7.2 Hz, 2H), 4.13 (q, J = 6.8 Hz, 2H), 4.02−3.95 (m, 3H), 3.84 (m, 1H), 3.54 (m, 2H), 3.26−2.97 (m, 7H), 2.76 (m, 1H), 2.62 (m, 2H), 2.17 (s, 3H), 2.15−1.86 (m, 5H), 1.78−1.54 (m, 8H), 1.48−1.20 (m, 35H), 1.03 (m, 1H). ESMS *m/z*: 942.7 (M+1).

(tert-Butoxycarbonyl-{3-[4-(2-{[1-(3-{tert-butoxycarbonyl-[3-(tert-butoxycarbonyl-cyclohexyl-amino)-propyl]-amino}-propyl)-1H-[1,2,3]triazol-4-ylmethyl]-amino}-6-

methyl-pyrimidin-4-ylamino)-piperidin-1-yl]-3-oxo-propyl}-amino)-acetic acid (15). To a solution of **14** (455 mg, 0.48 mmole) in THF (2.28 mL) under an atmosphere of nitrogen was added a solution of LiOH(aq) (1.37 mL, 1*N*). The mixture was stirred at 25 ^{o}C for 15 h and then quenched with NH_4Cl(aq). The aqueous phase was extracted with ethyl acetate. The combined organic extracts were washed with brine, dried over anhydrous sodium sulfate, filtered, and concentrated. The residue thus obtained was purified by flash chromatography on silica gel with MeOH/DCM (1:9) to give the compound **15** (435 mg, 99%) as sticky oil. ^{1}H NMR (400 MHz, CD_3OD) δ 7.88 (s, 1H), 5.72 (s, 1H), 4.62 (m, 2H), 4.41−4.36 (m, 3H), 4.08 (m, 1H), 3.96 (m, 1H), 3.81 (m, 2H), 3.54 (t, *J* = 6.8 Hz, 2H), 3.30−3.18 (m, 5H), 3.07 (m, 2H), 2.84 (m, 1H), 2.71 (m, 2H), 2.14 (s, 3H), 2.10 (m, 2H), 2.00−1.60 (m, 11H), 1.56−1.08 (m, 32H), 1.12 (m, 1H). ESMS *m/z*: 914.6 (M+1).

(3-{4-[2-({1-[3-(3-Cyclohexylamino-propylamino)-propyl]-1H-[1,2,3]triazol-4-ylmethyl}-amino)-6-methyl-pyrimidin-4-ylamino]-piperidin-1-yl}-3-oxo-propylamino)-acetic acid hydrochloride salt (16). A solution of 1*N* HCl/ether (7 mL) was added to the solution of **15** (421 mg, 0.46 mmole) in dichloromethane (14 mL). The mixture was stirred at 25 ^{o}C for 15 h and concentrated to afford **16** (333 mg, 95%). ^{1}H NMR (400 MHz, D_2O) δ 8.01 (s, 1H), 5.89 (s, 1H), 4.73 (m, 2H), 4.56 (t, *J* = 6.8 Hz, 2H), 4.26 (m, 1H), 4.11 (m, 1H), 4.01 (s, 2H), 3.86 (m, 1H), 3.42 (t, *J* = 6.0 Hz, 2H),

3.25 (m, 1H), 3.21−3.07 (m, 6H), 2.98 (t, *J* = 6.0 Hz, 2H), 2.90 (m, 1H), 2.33 (m, 2H), 2.24 (s, 3H), 2.18−2.04 (m, 5H), 1.96−1.78 (m, 4H), 1.67 (m, 1H), 1.51 (m, 1H), 1.41−1.16 (m, 6H). ^{13}C NMR (75 MHz, D_2O) δ 169.57, 169.01, 162.33, 153.85, 151.91, 145.68, 123.48, 96.50, 57.39, 47.61, 47.56, 47.27, 44.72, 44.56, 44.19, 43.76, 41.12, 40.71, 36.25, 30.34, 29.88, 28.74, 28.52, 26.16, 24.35, 23.77, 22.78, 17.62. ESMS *m/z*: 614.5 (M+1). HPLC purity = 97.45%, tR = 13.33 min.

3-(2-{4-[2-({1-[3-(3-Cyclohexylamino-propylamino)-propyl]-1H-[1,2,3]triazol-4-ylmethyl}-amino)-6-methyl-pyrimidin-4-ylamino]-piperidin-1-yl}-2-oxo-ethylamino)-propionic acid hydrochloride salt (17). Starting from compound **6** (301 mg, 0.44 mmole), compound **17** (193 mg) was obtained in 58% yield over three steps: ^{1}H NMR (400 MHz, D_2O) δ 8.03 (s, 1H), 5.92 (s, 1H), 4.75 (m, 2H), 4.58 (t, *J* = 6.8 Hz, 2H), 4.28−4.21 (m, 3H), 4.17 (m, 1H), 3.70 (m, 1H), 3.44 (t, *J* = 6.4 Hz, 2H), 3.28 (m, 1H), 3.21−3.08 (m, 6H), 2.99 (m, 1H), 2.94 (t, *J* = 6.4 Hz, 2H), 2.36 (m, 2H), 2.26 (s, 3H), 2.20−2.02 (m, 5H), 1.99−1.78 (m, 4H), 1.68 (m, 1H), 1.55 (m, 1H), 1.41−1.16 (m, 6H). ^{13}C NMR (75 MHz, D_2O) δ 174.03 , 163.62, 162.29, 153.79, 151.91, 145.69, 123.47, 96.47, 57.35, 47.79, 47.33, 47.24, 44.69, 44.54, 43.39, 43.19, 41.10, 41.06, 36.23, 30.10, 29.97, 29.67, 28.71, 26.16, 24.34, 23.76, 22.77, 17.61. ESMS *m/z*: 614.5 (M+1). HPLC purity = 96.71%, tR = 13.18 min.

(4-{4-[2-({1-[3-(3-Cyclohexylamino-propylamino)-propyl]-1H-[1,2,3]triazol-4-

ylmethyl}-amino)-6-methyl-pyrimidin-4-ylamino]-piperidin-1-yl}-4-oxo-butylamino)-acetic acid hydrochloride salt (18). Starting from compound **6** (304 mg, 0.44 mmole), compound **18** (199 mg) was obtained in 58% yield over three steps: ^{1}H NMR (400 MHz, D_2O) δ 7.99 (s, 1H), 5.89 (s, 1H), 4.73 (m, 2H), 4.56 (t, *J* = 6.4 Hz, 2H), 4.26 (m, 1H), 4.11 (m, 1H), 3.98 (s, 2H), 3.90 (m, 1H), 3.22 (m, 1H), 3.21−3.08 (m, 8H), 2.88 (m, 1H), 2.63 (t, *J* = 6.0 Hz, 2H), 2.32 (m, 2H), 2.24 (s, 3H), 2.18−1.98 (m, 7H), 1.97−1.74 (m, 4H), 1.66 (m, 1H), 1.49 (m, 1H), 1.41−1.16 (m, 6H). ^{13}C (75 MHz, D_2O) δ 172.20, 168.99, 162.29, 153.82, 151.86, 145.65, 123.45, 96.47, 57.36, 47.59, 47.30, 47.28, 46.93, 44.69, 44.54, 44.38, 41.09, 40.81, 36.20, 30.49, 29.99, 29.58, 28.71, 26.13, 24.34, 23.76, 22.77, 21.06, 17.59. ESMS *m/z*: 628.6 (M+1). HPLC purity = 97.81%, tR = 13.43 min.

3-(3-{4-[2-({1-[3-(3-Cyclohexylamino-propylamino)-propyl]-1H-[1,2,3]triazol-4-ylmethyl}-amino)-6-methyl-pyrimidin-4-ylamino]-piperidin-1-yl}-3-oxo-propylamino)-propionic acid hydrochloride salt (19). Starting from compound **6** (302 mg, 0.44 mmole), compound **19** (184 mg) was obtained in 54% yield over three steps. ^{1}H NMR (300 MHz, D_2O) δ 8.01 (s, 1H), 5.89 (s, 1H), 4.73 (m, 2H), 4.54 (t, *J* = 6.9 Hz, 2H), 4.25 (m, 1H), 4.11 (m, 1H), 3.86 (m, 1H), 3.42−3.35 (m, 4H), 3.24 (m, 1H), 3.21−3.06 (m, 6H), 2.95 (t, *J* = 6.0 Hz, 2H), 2.90−2.82 (m, 3H), 2.33 (m, 2H), 2.23 (s, 3H), 2.18−2.01 (m, 5H), 1.97−1.74 (m, 4H), 1.66 (m, 1H), 1.50 (m, 1H), 1.41−1.16 (m,

6H). ^{13}C (75 MHz, D_2O) δ 174.27, 169.77, 162.30, 153.82, 151.89, 145.62, 123.51, 96.50, 57.38, 47.53, 47.29, 44.71, 44.55, 44.14, 43.74, 42.96, 41.12, 40.69, 36.20, 30.32, 29.88, 29.70, 28.72, 28.26, 26.14, 24.35, 23.77, 22.78, 17.61. ESMS *m/z*: 628.6 (M+1). HPLC purity = 96.76%, tR = 13.37 min.

(3-{4-[2-({1-[3-(3-Cyclohexylamino-propylamino)-propyl]-1H-[1,2,3]triazol-4-ylmethyl}-amino)-6-ethyl-pyrimidin-4-ylamino]-piperidin-1-yl}-3-oxo-propylamino)-acetic acid hydrochloride salt (20). Starting from derivative of compound **6** (304 mg, 0.43 mmole), compound **20** (172 mg) was obtained in 51% yield over three steps: ^{1}H NMR (400 MHz, D_2O) δ 8.00 (s, 1H), 5.89 (s, 1H), 4.73 (m, 2H), 4.55 (t, *J* = 6.8 Hz, 2H), 4.24 (m, 1H), 4.10 (m, 1H), 4.00 (s, 2H), 3.85 (m, 1H), 3.41 (t, *J* = 6.0 Hz, 2H), 3.24 (m, 1H), 3.21−3.06 (m, 6H), 2.96 (t, *J* = 6.0 Hz, 2H), 2.88 (m, 1H), 2.52 (q, *J* = 7.6 Hz, 2H), 2.32 (m, 2H), 2.18−2.00 (m, 5H), 1.95−1.76 (m, 4H), 1.64 (m, 1H), 1.51 (m, 1H), 1.41−1.16 (m, 9H). ^{13}C NMR (100 MHz, D_2O) δ 169.63, 169.02, 162.56, 157.12, 153.97, 145.71, 123.56, 95.14, 57.44, 47.65, 47.63, 47.34, 44.77, 44.62, 44.22, 43.84, 41.19, 40.75, 36.31, 30.38, 29.92, 28.77, 28.57, 26.19, 25.11, 24.40, 23.82, 22.83, 10.86. ESMS *m/z*: 628.6 (M+1). HPLC purity = 95.28%, tR = 13.37 min.

(3-{4-[2-({1-[3-(3-Cyclohexylamino-propylamino)-propyl]-1H-[1,2,3]triazol-4-ylmethyl}-amino)-pyrimidin-4-ylamino]-piperidin-1-yl}-3-oxo-propylamino)-acetic acid hydrochloride salt (21). Starting from derivative of compound **6** (303 mg, 0.45

mmole), compound **21** (191 mg) was obtained in 57% yield over three steps: ^{1}H NMR (300 MHz, D_2O) δ 8.03 (s, 1H), 7.55 (d, *J* = 7.2 Hz, 1H), 6.09 (d, *J* = 7.2 Hz, 1H), 4.76 (m, 2H), 4.58 (t, *J* = 6.9 Hz, 2H), 4.28 (m, 1H), 4.16 (m, 1H), 3.97 (s, 2H), 3.89 (m, 1H), 3.44 (t, *J* = 6.0 Hz, 2H), 3.30 (m, 1H), 3.22−3.08 (m, 6H), 3.00 (t, *J* = 6.0 Hz, 2H), 2.92 (m, 1H), 2.36 (m, 2H), 2.19−2.02 (m, 5H), 1.98−1.78 (m, 4H), 1.68 (m, 1H), 1.55 (m, 1H), 1.41−1.17 (m, 6H). ^{13}C NMR (75 MHz, D_2O) δ 169.56, 169.17, 161.88, 153.34, 145.54, 140.00, 123.44, 98.14, 57.36, 47.77, 47.59, 47.21, 44.69, 44.54, 44.14, 43.70, 41.10, 40.67, 36.19, 30.19, 29.71, 28.71, 28.52, 26.16, 24.34, 23.76, 22.77. . ESMS *m/z*: 600.5 (M+1). HPLC purity = 97.63%, tR = 12.99 min.

[3-(4-{[2-({1-[3-(3-Cyclohexylamino-propylamino)-propyl]-1H-[1,2,3]triazol-4-ylmethyl}-amino)-6-methyl-pyrimidin-4-yl]-methyl-amino}-piperidin-1-yl)-3-oxo-propylamino]-acetic acid hydrochloride salt (22). Starting from derivative of compound **6** (302 mg, 0.43 mmole), compound **22** (164 mg) was obtained in 49% yield over three steps: ^{1}H NMR (300 MHz, D_2O) δ 8.02 (s, 1H), 6.15 (s, 1H), 4.75 (s, 2H), 4.60−4.40 (m, 4H), 4.00 (s, 2H), 3.98 (m, 1H), 3.44 (t, *J* = 6.0 Hz, 2H), 3.22−3.08 (m, 7H), 2.98 (m, 2H), 2.96 (s, 3H), 2.70 (m, 1H), 2.41−2.21 (m, 5H), 2.20−1.98 (m, 5H), 1.97−1.76 (m, 4H), 1.72−1.49 (m, 2H), 1.41−1.16 (m, 6H). ^{13}C NMR (75 MHz, D_2O) δ 169.57, 169.02, 161.97, 153.34, 152.66, 145.91, 123.40, 94.37, 57.38, 52.95, 47.65, 47.27, 44.83, 44.69, 44.57, 43.76, 41.39, 41.13, 36.43, 30.37, 29.51, 28.72, 28.58, 27.88,

26.19, 24.37, 23.79, 22.80, 18.10. ESMS *m/z*: 628.6 (M+1). HPLC purity = 95.95%, tR = 13.51 min.

5-{4-[2-({1-[3-(3-Cyclohexylamino-propylamino)-propyl]-1H-[1,2,3]triazol-4-ylmethyl}-amino)-6-methyl-pyrimidin-4-ylamino]-piperidin-1-yl}-5-oxo-pentanoic acid hydrochloride salt (23). Starting from compound **6** (305 mg, 0.45 mmole), compound **23** (163 mg) was obtained in 52% yield over three steps: ^{1}H NMR (300 MHz, D_2O) δ 8.03 (s, 1H), 5.89 (s, 1H), 4.73 (m, 2H), 4.56 (t, *J* = 6.6 Hz, 2H), 4.23 (m, 1H), 4.08 (m, 1H), 3.92 (m, 1H), 3.24 (m, 1H), 3.20−3.04 (m, 6H), 2.85 (m, 1H), 2.55−2.40 (m, 4H), 2.33 (m, 2H), 2.23 (s, 3H), 2.18−2.02 (m, 5H), 1.93−1.76 (m, 6H), 1.65 (m, 1H), 1.49 (m, 1H), 1.41−1.16 (m, 6H). ^{13}C NMR (75 MHz, D_2O) δ 177.71, 173.46, 162.30, 153.79, 151.91, 145.72, 123.57, 96.52, 57.38, 47.70, 47.36, 44.69, 44.62, 44.57, 41.13, 40.74, 36.19, 32.84, 31.74, 30.64, 30.02, 28.72, 26.13, 24.35, 23.77, 22.78, 20.22, 17.64. ESMS *m/z*: 599.5 (M+1). HPLC purity = 98.67%, tR = 12.90 min.

2-Amino-5-{4-[2-({1-[3-(3-cyclohexylamino-propylamino)-propyl]-1H-[1,2,3]triazol-4-ylmethyl}-amino)-6-methyl-pyrimidin-4-ylamino]-piperidin-1-yl}-5-oxo-pentanoic acid hydrochloride salt (24). Starting from compound **6** (302 mg, 0.44 mmole), compound **24** (179 mg) was obtained in 53% yield over two steps: ^{1}H NMR (300 MHz, D_2O) δ 8.04 (s, 1H), 6.01 (s, 1H), 4.74 (m, 2H), 4.56 (t, *J* = 6.9 Hz, 2H), 4.30 (m, 1H), 4.12−4.00 (m, 2H), 3.92 (m, 1H), 3.25 (m, 1H), 3.21−3.06 (m, 6H), 2.88 (m,

1H), 2.71 (t, *J* = 6.6 Hz, 2H), 2.34 (m, 2H), 2.26 (s, 3H), 2.23 (m, 2H), 2.18−2.02 (m, 5H), 1.99−1.80 (m, 4H), 1.68 (m, 1H), 1.54 (m, 1H), 1.42−1.18 (m, 6H). ^{13}C NMR (75 MHz, D_2O) δ 171.68, 171.54, 163.17, 153.16, 152.33, 145.17, 123.66, 96.21, 57.38, 52.14, 47.96, 47.29, 44.69, 44.54, 44.40, 41.10, 40.89, 35.90, 30.69, 30.19, 28.71, 28.45, 26.11, 25.26, 24.34, 23.76, 22.77, 17.68. ESMS *m/z*: 614.5 (M+1). HPLC purity = 96.21%, tR = 13.30 min.

[(3-{4-[2-({1-[3-(3-Cyclohexylamino-propylamino)-propyl]-1H-[1,2,3]triazol-4-ylmethyl}-amino)-6-methyl-pyrimidin-4-ylamino]-piperidin-1-yl}-3-oxo-propylamino)-methyl]-phosphonic acid hydrobromide salt (25). Starting from compound **6** (302 mg, 0.44 mmole), compound **25** (224 mg) was obtained in 57% yield over two steps: ^{1}H NMR (300 MHz, D_2O) δ 8.02 (s, 1H), 5.88 (s, 1H), 4.73 (m, 2H), 4.56 (t, *J* = 6.9 Hz, 2H), 4.22 (m, 1H), 4.10 (m, 1H), 3.84 (m, 1H), 3.45 (t, *J* = 6.3 Hz, 2H), 3.31−3.04 (m, 9H), 2.96 (t, *J* = 6.3 Hz, 2H), 2.88 (m, 1H), 2.33 (m, 2H), 2.23 (s, 3H), 2.08−2.00 (m, 5H), 1.96−1.70 (m, 4H), 1.65 (m, 1H), 1.51 (m, 1H), 1.41−1.17 (m, 6H). ^{13}C NMR (75 MHz, D_2O) δ 169.74, 162.30, 153.80, 151.88, 145.60, 123.56, 96.52, 57.35, 47.54, 47.32, 45.27, 44.71, 44.55, 44.20, 42.84, 41.12, 40.67, 36.23, 30.29, 29.83, 28.72, 28.20, 26.14, 24.34, 23.76, 22.77, 17.63 . ESMS *m/z*: 650.6 (M+1). HPLC purity = 97.01%, tR = 13.26 min.

[2-(3-{4-[2-({1-[3-(3-Cyclohexylamino-propylamino)-propyl]-1H-[1,2,3]triazol-4-

ylmethyl}-amino)-6-methyl-pyrimidin-4-ylamino]-piperidin-1-yl}-3-oxo-propylamino)-ethyl]-phosphonic acid hydrobromide salt (26). Starting from compound **6** (300 mg, 0.44 mmole), compound **26** (214 mg) was obtained in 54% yield over two steps: ^{1}H NMR (300 MHz, D_2O) δ 8.03 (s, 1H), 5.90 (s, 1H), 4.75 (m, 2H), 4.58 (t, *J* = 6.9 Hz, 2H), 4.25 (m, 1H), 4.12 (m, 1H), 3.86 (m, 1H), 3.41−3.30 (m, 4H), 3.24−3.06 (m, 7H), 2.96−2.90 (m, 3H), 2.88 (t, *J* = 6.6 Hz, 2H), 2.35 (m, 2H), 2.25 (s, 3H), 2.20−2.02 (m, 5H), 1.97−1.74 (m, 4H), 1.65 (m, 1H), 1.52 (m, 1H), 1.41−1.16 (m, 6H). ^{13}C (75 MHz, D_2O) δ 169.51, 162.29, 153.79, 151.88, 145.34, 123.86, 96.60, 57.36, 47.54, 47.50, 44.69, 44.57, 44.16, 43.41, 42.75, 41.15, 40.69, 36.14, 30.35, 29.96, 29.88, 28.72, 28.61, 26.10, 24.34, 23.76, 22.78, 17.67. ESMS *m/z*: 664.6 (M+1). HPLC purity = 96.54%, tR = 13.48 min.

N2-{1-[3-(3-Cyclohexylamino-propylamino)-propyl]-1H-[1,2,3]triazol-4-ylmethyl}-6-methyl-N4-(1-propyl-piperidin-4-yl)-pyrimidine-2,4-diamine hydrochloride salt (27). Starting from compound **6** (301 mg, 0.44 mmole), compound **27** (176 mg) was obtained in 59% yield over two steps: ^{1}H NMR (300 MHz, D_2O) δ 8.01 (s, 1H), 6.01 (s, 0.2H), 5.92 (s, 0.8H), 4.75 (s, 2H), 4.56 (t, *J* = 6.6 Hz, 2H), 4.28 (m, 0.2H), 4.17 (m, 0.8H), 3.64 (m, 1.6H), 3.46 (m, 0.4H), 3.21−3.04 (m, 10H), 2.33 (m, 2H), 2.26 (s, 3H), 2.18−2.00 (m, 6H), 1.90−1.62 (m, 7H), 1.40−1.17 (m, 6H), 0.99 (t, *J* = 7.5 Hz, 3H). ^{13}C NMR (75 MHz, D_2O) δ 162.59, 153.86, 152.29, 145.72, 123.48, 96.47, 58.35, 57.38,

51.42, 47.19, 45.51, 44.71, 44.54, 41.10, 36.22, 28.72, 28.08, 26.16, 24.34, 23.76, 22.78, 17.62, 17.19, 10.05. ESMS *m/z*: 527.5 (M+1). HPLC purity = 98.68%, tR = 13.52 min.

3-{4-[2-({1-[3-(3-Cyclohexylamino-propylamino)-propyl]-1H-[1,2,3]triazol-4-ylmethyl}-amino)-6-methyl-pyrimidin-4-ylamino]-piperidin-1-yl}-propionitrile trifluoro acetic acid salt (28). Starting from compound **6** (303 mg, 0.44 mmole), compound **28** (260 mg) was obtained in 59% yield over two steps: ^{1}H NMR (300 MHz, D_2O) δ 7.94 (s, 1H), 5.92 (s, 0.24H), 5.82 (s, 0.76H), 4.67 (s, 2H), 4.47 (t, *J* = 7.2 Hz, 2H), 4.20 (m, 0.24H), 4.09 (m, 0.76H), 3.63 (m, 1.52H), 3.57−3.46 (m, 2.48H), 3.17−3.02 (m, 10H), 2.25 (m, 2H), 2.16 (s, 3H), 2.14−1.96 (m, 6H), 1.80−1.58 (m, 5H), 1.34−1.02 (m, 6H). ^{13}C NMR (75 MHz, D_2O) δ 162.52, 162.42 (q, *J* = 35.5 Hz, $CF_3\underline{C}O_2H$), 153.75, 152.29, 145.27, 123.71, 117.30, 116.00 (q, *J* = 289.7 Hz, $\underline{C}F_3CO_2H$), 96.49, 57.28, 51.76, 51.32, 47.41, 45.10, 44.55, 44.42, 40.96, 35.88, 28.61, 27.74, 27.42, 25.91, 24.23, 23.67, 22.66, 17.45. ESMS *m/z*: 538.5 (M+1). HPLC purity = 97.34%, tR = 13.52 min.

3-{4-[2-({1-[3-(3-Cyclohexylamino-propylamino)-propyl]-1H-[1,2,3]triazol-4-ylmethyl}-amino)-6-methyl-pyrimidin-4-ylamino]-piperidin-1-yl}-propionamide hydrochloride salt (29). Starting from compound **6** (301 mg, 0.44 mmole), compound **29** (181 mg) was obtained in 59% yield over two steps: ^{1}H NMR (300 MHz, D_2O) δ 8.02 (s, 1H), 6.02 (s, 0.22H), 5.93 (s, 0.78H), 4.76 (m, 2H), 4.57 (t, *J* = 6.9 Hz, 2H), 4.25

(m, 0.22H), 4.19 (m, 0.78H), 3.68 (m, 1.56H), 3.56−3.46 (m, 2.44H), 3.23−3.10 (m, 8H), 2.86 (t, *J* = 6.6 Hz, 2H), 2.35 (m, 2H), 2.27 (s, 3H), 2.20−12.03 (m, 6H), 1.90−1.62 (m, 5H), 1.42−1.18 (m, 6H). ^{13}C NMR (75 MHz, D_2O) δ 174.06, 162.62, 153.88, 152.35, 145.71, 123.51, 96.50, 57.39, 52.45, 51.76, 47.21, 45.35, 44.74, 44.55, 41.12, 36.22, 29.04, 28.72, 28.03, 26.16, 24.35, 23.77, 22.78, 17.64. ESMS *m/z*: 556.5 (M+1). HPLC purity = 96.01%, tR = 13.25 min.

3-{4-[2-({1-[3-(3-Cyclohexylamino-propylamino)-propyl]-1H-[1,2,3]triazol-4-ylmethyl}-amino)-6-methyl-pyrimidin-4-ylamino]-piperidin-1-yl}-propionic acid hydrochloride salt (30). Starting from compound **6** (299 mg, 0.44 mmole), compound **30** (188 mg) was obtained in 61% yield over two steps: ^{1}H NMR (400 MHz, D_2O) δ 8.01 (s, 1H), 6.01 (s, 0.22H), 5.91 (s, 0.78H), 4.75 (s, 2H), 4.55 (t, *J* = 6.8 Hz, 2H), 4.24 (m, 0.22H), 4.18 (m, 0.78H), 3.66 (m, 1.56H), 3.55−3.46 (m, 2.44H), 3.23−3.08 (m, 8H), 2.94 (t, *J* = 6.8 Hz, 2H), 2.33 (m, 2H), 2.25 (s, 3H), 2.18−2.02 (m, 6H), 1.90−1.62 (m, 5H), 1.42−1.17 (m, 6H). ^{13}C NMR (75 MHz, D_2O) δ 173.69, 162.62, 153.86, 152.33, 145.71, 123.51, 96.50, 57.39, 52.09, 51.87, 47.22, 45.35, 44.74, 44.55, 41.12, 36.23, 28.72, 28.66, 27.99, 26.16, 24.35, 23.77, 22.80, 17.64 . ESMS *m/z*: 557.5 (M+1). HPLC purity = 95.58%, tR = 13.07 min.

5-{4-[2-({1-[3-(3-Cyclohexylamino-propylamino)-propyl]-1H-[1,2,3]triazol-4-ylmethyl}-amino)-6-methyl-pyrimidin-4-ylamino]-piperidin-1-yl}-pentanoic acid

hydrochloride salt (31). Starting from compound **6** (298 mg, 0.44 mmole), compound **31** (160 mg) was obtained in 50% yield over three steps: ^{1}H NMR (400 MHz, D_2O) δ 8.00 (s, 1H), 6.02 (s, 0.23H), 5.93 (s, 0.77H), 4.76 (s, 2H), 4.56 (t, *J* = 6.4 Hz, 2H), 4.25 (m, 0.23H), 4.19 (m, 0.77H), 3.65 (m, 1.54H), 3.48 (m, 0.46H), 3.30−3.06 (m, 10H), 2.49 (t, *J* = 6.4 Hz, 2H), 2.35 (m, 2H), 2.27 (s, 3H), 2.20−2.03 (m, 6H), 1.95−1.64 (m, 9H), 1.42−1.17 (m, 6H). ^{13}C NMR (100 MHz, D_2O) δ 177.92, 162.57, 153.84, 152.28, 145.61, 123.47, 96.46, 57.36, 56.32, 51.49, 47.18, 45.46, 44.71, 44.53, 41.09, 36.21, 32.83, 28.70, 28.06, 26.14, 24.33, 23.76, 22.91, 22.78, 21.09, 17.59. ESMS *m/z*: 585.5 (M+1). HPLC purity = 98.30%, tR = 13.28 min.

7-{4-[2-({1-[3-(3-Cyclohexylamino-propylamino)-propyl]-1H-[1,2,3]triazol-4-ylmethyl}-amino)-6-methyl-pyrimidin-4-ylamino]-piperidin-1-yl}-heptanoic acid hydrochloride salt (32). Starting from compound **6** (302 mg, 0.44 mmole), compound **32** (153 mg) was obtained in 47% yield over three steps: ^{1}H NMR (300 MHz, D_2O) δ 8.02 (s, 1H), 6.03 (s, 0.2H), 5.93 (s, 0.8H), 4.76 (s, 2H), 4.57 (t, *J* = 6.3 Hz, 2H), 4.24 (m, 0.2H), 4.18 (m, 0.8H), 3.65 (m, 1.6H), 3.48 (m, 0.4H), 3.30−3.02 (m, 10H), 2.45 (t, *J* = 6.9 Hz, 2H), 2.37 (m, 2H), 2.26 (s, 3H), 2.20−2.00 (m, 6H), 1.97−1.60 (m, 9H), 1.50−1.13 (m, 8H). ^{13}C NMR (75 MHz, D_2O) δ 178.61, 162.59, 153.86, 152.32, 145.74, 123.53, 96.50, 57.38, 56.61, 51.47, 47.22, 45.51, 44.72, 44.55, 41.12, 36.23, 33.30, 28.72, 28.1, 26.16, 25.10, 24.35, 23.77, 23.55, 23.19, 22.78, 17.64. ESMS *m/z*: 599.6

(M+1). HPLC purity = 97.55%, tR = 13.42 min.

Animals. Eight to ten week-old male C57BL/6 mice were used in the study of stem/progenitor cell counting. Male Sprague–Dawley rats (weighing approximately 200-250 g) were used in the study of AKI. All animals were purchased from National Laboratory Animals Center (Taipei, Taiwan, R.O.C.). The Institutional Animal Care and Use Committee (IACUC) of National Health Research Institutes (NHRI) approved all experimental protocols.

Establishment of Human CXCR4 Stable Cell Line and Membrane Purification. The hCXCR4 cDNA was subcloned into pIRES2-EGFP vector (Clontech Laboratories, Inc., Mountain View, CA). Transfected HEK-293 cells stably expressed hCXCR4 (HEK-293 CXCR4) were selected by EGFP and 1 mg/mL G418 sulfate. The selected clone was maintained in DMEM supplemented with 10% fetal bovine serum and 0.5 mg/mL G418 sulfate with 5% CO_2 at 37 ^{o}C in the humidified incubator. For membrane purification, cells were homogenized in ice-cold buffer A (50 mM Tris-HCl, pH 7.4, 5 mM $MgCl_2$, 2.5 mM EDTA, 10% sucrose) with freshly prepared 1 mM PMSF. The homogenate was centrifuged at 3500 x g for 15 min at 4 ^{o}C. The pellet was removed and the supernatant then was centrifuged at 43000 x g for additional 30 min at 4 ^{o}C. The final pellet was resuspended in buffer A and stored at -80 ^{o}C.

Radioligand Binding Assay. An amount of 2–4 μg of purified membrane with CXCR4

was incubated with 0.16 nM [^{125}I]CXCL12 and compounds of interest in the incubation buffer (50 mM HEPES-NaOH, pH 7.4, 100 mM NaCl, 5 mM $MgCl_2$, 1 mM $CaCl_2$, 0.5% BSA) The nonspecific binding was defined in the presence of 50 μM AMD3100 (plerixafor). The reaction mixtures were incubated for 1.5 h at 30 ^{o}C and then were transferred to a 96-well GF/B filter plate (Millipore Corp., Billerica, MA, USA). The reaction mixtures were terminated by maniford filtration and washed with ice-cold wash buffer (50 mM HEPES-NaOH, pH 7.4, 100 mM NaCl) for four times. The radioactivity bound to the filter was measured by Topcount (PerkinElmer Inc., Waltham, MA, USA). IC_{50} values were determined by the concentration of compounds required to inhibit 50% of the specific binding of [^{125}I]SDF-1 and calculated by nonlinear regression (GraphPad software, San Diego, CA, USA).

Chemotaxis Assay. CCRF-CEM (T-cell acute lymphoblastic leukemia) cells were suspended in RPMI 1640 containing 10% FBS and then preincubated with indicated concentrations of compounds for 10 min at 37 ^{o}C. The assay was performed in Millicell Hanging Cell Culture Inserts (pore size 5 μm; 24-well plate; Millipore, Bedford, MA, USA). Compounds containing 10 nM CXCL12 were plated in the lower chambers of inserts, and cells with compounds were plated in the upper chambers of inserts at a density of 2.5×10^5 cells/well. After 2.5 h incubation at 37 ^{o}C, cells in both chambers of inserts were measured by flow cytometer (Guava Technologies, Hayward, CA, USA).

Flow Cytometry Analysis for Stem/Progenitor Cell Counting. C57BL/6 male mice were treated with potential CXCR4 antagonist individually by subcutaneous injection, and then blood samples containing mobilized stem/progenitor cells were collected 2 hours later. After labeled with specific antibodies, including APC-conjugated anti-CXCR4 (clone 2B11; eBioscience), FITC-conjugated anti-CD34 (clone RAM34; eBioscience), PE-conjugated anti-CD133 (clone 13A4; eBioscience) and anti-VEGFR2 (clone Avsa12a1; eBioscience), anti-Sca-1 (clone D7; eBioscience), cells were washed, characterized and quantified by flow cytometer (Guava Technologies, Hayward, CA, USA). Each data point included at least 60,000 events for analysis of different cell types.

Efficacy Analyzed by Colony-Forming Assay. C57BL/6 male mice were treated with 100 μg/kg G-CSF for 5 consecutive days by SC injection. The mice were treated with indicated concentrations of compounds **1** or **16** individually on day 5 by SC injection, and then blood samples containing mobilized stem cells were collected 2 h later. The heparinized blood sample was collected and peripheral blood mononuclear cells (PBMCs) were isolated and cultured in methylcellulose medium (MethoCult GF M3434). CFU-GM colonies were counted after 10–14 days of incubation under an inverted microscope. The aggregate of more than 50 cells was recorded as a colony.

Plasma Pharmacokinetics in mice. Male C57BL/6, each weighing 23.4–25.4 g, were quarantined for one week before treatment. Compounds **1** and **16**, dissolved in 100% saline, were individually given to mice (n = 3) subcutaneously (6 mg/kg; non-fasted

mice). Blood samples were collected via the cardiac puncture at defined time points, 0 (immediately before dosing), 0.03, 0.08, 0.25, 1, 1.5, 2 and 4 h after dosing, and then stored at -80 ^{o}C. The volume of the dosing solution given was 100 μL for each mouse. The plasma samples were analyzed by liquid chromatography–tandem mass spectrometry (LC–MS/MS) and data were calculated by a standard non-compartmental method using the Kinetica software program (InnaPhase, USA).

Acute Toxicology Study. C57BL/6 or ICR male mice were subcutaneously treated with test compounds (n = 3/group) from a low to high dose to determine maximum tolerated dose (MTD) based on zero mortality (n = 3, 0/3).

Docking analysis with the CXCR4 crystal structure. Binding interactions between the CXCR4 crystal structure (PDB ID: 4RWS) and compound **16** were illustrated through docking and molecular dynamics (MD) simulations. For the docking calculation, the mutated residues (L125W, D187C, and T240P) have been restored to original ones. Through conformational analysis of compound **16**, the best pose was chosen for further MD simulations. After 20 ns simulations, the complex structure in an equilibrium and stable state was shown in Figures 1 and 2. All calculations were performed by means of Discovery Studio 2017 software (BIOVIA, Inc., San Diego, CA). The docking analysis was conducted using the DS/LigandFit program with the CHARMm force field.[52] The number of docking poses was set as 100 with default parameters.

Molecular dynamics simulation of compound 16. The molecular dynamics (MD) simulations were carried out using GROMACS v5.1.2 to refine the docked

conformation.[53] The topology of docked ligand **16** was generated by PRODRG serve.[54] The force field for the whole system was GROMOS 43a1.[55] The protein-ligand complex was restrained in a box of cubic shape whose edges were placed at 1 nm from the complex and SPC/E water model was performed. The system was electrically neutralized by adding 5 NA^+ ion. The energy minimization was performed using steepest descent and conjugate gradient algorithms to converge the system up to 10 kJ $mol^{-1}nm^{-1}$. After the above short energy minimization step, the system was subjected to NVT (300K) and NPT (1 bar) equilibration with 100 ps running, and LINCS algorithm was used to constrain the hydrogen bond lengths.[56] The time step was kept 2 fs for the simulation. The cut-off distance of 10 Å was used for all short range non-bonded interactions and 12 Å Fourier grid spacing in PME method for long range electrostatics. Finally, the hydrogen bond constraints of the protein-ligand complex were removed and performed to a 20 ns MD simulation.

Statistical Analysis. Apart from chemotaxis assay, which is presented as mean ± standard deviation (SD), other values are expressed as mean ± standard error of the mean (SEM). The results were analyzed by Student's *t*-test. For all comparisons between groups, $p < 0.05$ was considered statistically significant.

ASSOCIATED CONTENT

Supporting Information

The Supporting Information is available free of charge on the ACS Publications website at http://pubs.acs.org.

Compound **16**'s off-target and patch-clamp assays by Eurofins Panlabs Taiwan, Ltd.; counter screening against 12 chemokine receptors by DiscoverX Corporation, Fremont, CA 94538; synthetic protocols of linkers and their characterization data; copies of ^{1}H and ^{13}C NMR spectra of representative compounds **7-10** and **16-21** are included (PDF)

Binding model of **16** in CXCR4 receptor (PDB)

Molecular formula strings of all target compounds (CSV)

AUTHOR INFORMATION

Corresponding Author

*Telephone: +886-37-246-166 ext. 35709. Fax: +886-37-586-456. E-mail: ksshia@nhri.org.tw

ORCID

Chien-Huang Wu: 0000-0002-9416-801X

Hsuan-Hao Kuan: 0000-0001-9782-9402

Lun K. Tsou: 0000-0002-1593-5226

Kak-Shan Shia: 0000-0001-9560-2466

Author Contributions

†These authors contributed equally to this work.

Notes

The authors declare no competing financial interest.

ACKNOWLEDGMENTS

We are grateful to the National Health Research Institutes and Ministry of Science and Technology of the Republic of China (MOST 101-2325-B-400-016) for financial support.

ABBREVIATIONS USED

CXCR4, G protein-coupled CXC chemokine receptor 4; SDF-1, stromal cell-derived factor-1; G-CSF, granulocyte colony-stimulating factor; HSCs, hematopoietic stem cells; EPCs, endothelial progenitor cells; MSCs, mesenchymal stem cells; MTD, maximum tolerated dose; SC, subcutaneous; SAR, structure-activity relationship; SD, standard deviation; SEM, standard error of the mean; ESMS, electrospray mass spectra

Authors will release the atomic coordinates and experimental data upon article publication.

REFERENCES

1. Lipfert, J.; Odemis, V.; Wagner, D. C.; Boltze, J.; Engele, J. CXCR4 and CXCR7 form a functional receptor unit for SDF-1/CXCL12 in primary rodent microglia. *Neuropathol. Appl. Neurobiol.* **2013**, *39*, 667–680.

2. Robin, A. M.; Zhang, Z. G.; Wang, L.; Zhang, R. L.; Katakowski, M.; Zhang, L.; Wang, Y.; Zhang, C.; Chopp, M. Stromal cell-derived factor 1alpha mediates neural progenitor cell motility after focal cerebral ischemia. *J. Cereb. Blood Flow Metab.* **2006**, *26*, 125–134.

3. Stumm, R. K.; Rummel, J.; Junker, V.; Culmsee, C.; Pfeiffer, M.; Krieglstein, J.; Hollt, V.; Schulz, S. A dual role for the SDF-1/CXCR4 chemokine receptor system in adult brain: isoform-selective regulation of SDF-1 expression modulates CXCR4-dependent neuronal plasticity and cerebral leukocyte recruitment after focal ischemia. *J. Neurosci.* **2002**, *22*, 5865–5878.

4. Tran, P. B.; Banisadr, G.; Ren, D.; Chenn, A.; Miller, R. J. Chemokine receptor expression by neural progenitor cells in neurogenic regions of mouse brain. *J. Comp. Neurol.* **2007**, *500*, 1007–1033.

5. Li, M.; Ransohoff, R. M. Multiple roles of chemokine CXCL12 in the central nervous system: a migration from immunology to neurobiology. *Prog. Neurobiol.* **2008**, *84*, 116–131.

6. Lapidot, T.; Dar, A.; Kollet, O. How do stem cells find their way home? *Blood* **2005**, *106*, 1901–1910.

7. Pitchford, S. C.; Furze, R. C.; Jones, C. P.; Wengner, A. M.; Rankin, S. M. Differential mobilization of subsets of progenitor cells from the bone marrow. *Cell Stem Cell* **2009**, *4*, 62–72.

8. Liu, X.; Duan, B.; Cheng, Z.; Jia, X.; Mao, L.; Fu, H.; Che, Y.; Ou, L.; Liu, L.; Kong, D. SDF-1/CXCR4 axis modulates bone marrow mesenchymal stem cell apoptosis, migration and cytokine secretion. *Protein Cell* **2011**, *2*, 845–854.

9. For recent reviews, see: (a) Tsou, L. K.; Huang, Y. H.; Song, J. S.; Ke, Y. Y.; Huang, J. K.; Shia, K. S. Harnessing CXCR4 Antagonists in Stem Cell Mobilization, HIV Infection, Ischemic Diseases and Oncology. *Med. Res. Rev.* [Online early access]. DOI: 10.1002/med.21464. Published Online: Aug 2, 2017. https://www.ncbi.nlm.nih.gov/pubmed/28768055 (accessed Aug 2, 2017). (b) Choi, W. T.; Duggineni, S.; Xu, Y.; Huang, Z.; An, J. Drug discovery research targeting the CXC chemokine receptor 4 (CXCR4). *J. Med. Chem.* **2012**, *55*, 977–994.

10. Fiorina, P.; Jurewicz, M.; Vergani, A.; Petrelli, A.; Carvello, M.; D'Addio, F.; Godwin, J. G.; Law, K.; Wu, E.; Tian, Z.; Thoma, G.; Kovarik, J.; La Rosa, S.; Capella, C.; Rodig, S.; Zerwes, H. G.; Sayegh, M. H.; Abdi, R. Targeting the CXCR4-CXCL12 axis mobilizes autologous hematopoietic stem cells and prolongs islet allograft survival via programmed death ligand 1. *J. Immunol.* **2011**, *186*, 121–131.

11. Ben Nasr, M.; Fiorina, P. CXCR4 antagonism overcomes diabetic stem cell mobilopathy. *Atherosclerosis* **2016**, *251*, 512–513.

12. Gulick, R. M.; Lalezari, J.; Goodrich, J.; Clumeck, N.; DeJesus, E.; Horban, A.; Nadler, J.; Clotet, B.; Karlsson, A.; Wohlfeiler, M.; Montana, J. B.; McHale, M.; Sullivan, J.; Ridgway, C.; Felstead, S.; Dunne, M. W.; van der Ryst, E.; Mayer, H.; Teams, M. S. Maraviroc for previously treated patients with R5 HIV-1 infection. *N. Engl. J. Med.* **2008**, *359*, 1429–1441.

13. Westby, M.; Lewis, M.; Whitcomb, J.; Youle, M.; Pozniak, A. L.; James, I. T.; Jenkins, T. M.; Perros, M.; van der Ryst, E. Emergence of CXCR4-using human immunodeficiency virus type 1 (HIV-1) variants in a minority of HIV-1-infected patients following treatment with the CCR5 antagonist maraviroc is from a pretreatment CXCR4-using virus reservoir. *J. Virol.* **2006**, *80*, 4909–4920.

14. Hendrix, C. W.; Collier, A. C.; Lederman, M. M.; Schols, D.; Pollard, R. B.; Brown, S.; Jackson, J. B.; Coombs, R. W.; Glesby, M. J.; Flexner, C. W.; Bridger, G. J.; Badel, K.; MacFarland, R. T.; Henson, G. W.; Calandra, G. Safety, pharmacokinetics, and antiviral activity of AMD3100, a selective CXCR4 receptor inhibitor, in HIV-1 infection. *J. Acquired Immune Defic. Syndr.* **2004**, *37*, 1253–1262.

15. Nyunt, M. M.; Becker, S.; Macfarland, R. T.; Chee, P.; Scarborough, R.; Everts, S.; Calandra, G. B.; Hendrix, C. W. Pharmacokinetic Effect of AMD070, an oral CXCR4

antagonist, on CYP3A4 and CYP2D6 substrates midazolam and dextromethorphan in healthy volunteers. *J. Acquir. Immune Defic. Syndr.* **2008**, *47*, 559–565.

16. Moyle, G.; DeJesus, E.; Boffito, M.; Wong, R. S.; Gibney, C.; Badel, K.; MacFarland, R.; Calandra, G.; Bridger, G.; Becker, S. Proof of activity with AMD11070, an orally bioavailable inhibitor of CXCR4-tropic HIV type 1. *Clin. Infect. Dis.* **2009**, *48*, 798–805.

17. (a) Murakami, T.; Kumakura, S.; Yamazki, T.; Tanaka, R.; Hamatake, M.; Okuma, K.; Huang, W.; Toma, J.; Komano, J.; Yanaka, M.; Tanaka, Y.; Yamamoto, N. The novel CXCR4 antagonist KRH-3955 is an orally bioavailable and extremely potent inhibitor of human immunodeficiency virus type 1 infection: comparative studies with AMD3100. *Antimicrob. Agents Chemother.* **2009**, *53*, 2940–2948. (b) Zachariassen, Z. G.; Karlshøj, S.; Haug, B. E.; Rosenkilde, M. M.; Våbenø, J. Probing the molecular interactions between CXC chemokine receptor 4 (CXCR4) and an arginine-based tripeptidomimetic antagonist (KRH-1636). *J. Med. Chem.* **2015**, *58*, 8141−8153.

18. Schols, D.; Struyf, S.; Van Damme, J.; Esté, J. A.; Henson, G.; De Clercq, E. Inhibition of T-tropic HIV strains by selective antagonization of the chemokine receptor CXCR4. *J. Exp. Med.* **1997**, *186*, 1383–1388.

19. Wu, C. H.; Wang, C. J.; Chang, C. P.; Cheng, Y. C.; Song, J. S.; Jan, J. J.; Chou, M. C.; Ke, Y. Y.; Ma, J.; Wong, Y. C.; Hsieh, T. C.; Tien, Y. C.; Gullen, E. A.; Lo, C. F.; Cheng, C. Y.; Liu, Y. W.; Sadani, A. A.; Tsai, C. H.; Hsieh, H. P.; Tsou, L. K.; Shia, K. S. Function-oriented development of CXCR4 antagonists as selective human immunodeficiency virus (HIV)-1 entry inhibitors. *J. Med. Chem.* **2015**, *58*, 1452–1465.

20. Wang, Y.; Deng, Y.; Zhou, G. Q. SDF-1alpha/CXCR4-mediated migration of systemically transplanted bone marrow stromal cells towards ischemic brain lesion in a rat model. *Brain Res.* **2008**, *1195*, 104–112.

21. Borlongan, C. V.; Hida, H.; Nishino, H. Early assessment of motor dysfunctions aids in successful occlusion of the middle cerebral artery. *Neuroreport.* **1998**, *9*, 3615–3621.

22. Wu, K. J.; Yu, S. J.; Shia, K. S.; Wu, C. H.; Song, J. S.; Kuan, H. H.; Yeh, K. C.; Chen, C. T.; Bae, E.; Wang Y. A novel CXCR4 antagonist CX549 induces neuroprotection in stroke brain. *Cell Transplant.* **2017**, *26*, 571–583.

23. Wu, C. H.; Song, J. S.; Chang, K. H.; Jan, J. J.; Chen, C. T.; Chou, M. C.; Yeh, K. C.; Wong, Y. C.; Tseng, C. T.; Wu, S. H.; Yeh, C. F.; Huang, C. Y.; Wang, M. H.; Sadani, A. A.; Chang, C. P.; Cheng, C. Y.; Tsou, L. K.; Shia, K. S. Stem cell mobilizers

targeting chemokine receptor CXCR4: renoprotective application in acute kidney injury. *J. Med. Chem.* **2015**, *58*, 2315–2325.

24. Luo, Y.; Zhao, X.; Zhou, X.; Ji, W.; Zhang, L.; Luo, T.; Liu, H.; Huang, T.; Jiang, T.; Li, Y. Short-term intermittent administration of CXCR4 antagonist AMD3100 facilitates myocardial repair in experimental myocardial infarction. *Acta Biochim. Biophys. Sin.* **2013**, *45*, 561–569.

25. Hsu, W. T.; Jui, H. Y.; Huang, Y. H.; Su, M. Y. M.; Wu, Y. W.; Tseng, W. Y. I.; Hsu, M. C.; Chiang, B. L.; Wu, K. K.; Lee, C. M. CXCR4 antagonist TG-0054 mobilizes mesenchymal stem cells, attenuates inflammation, and preserves cardiac systolic function in a porcine model of myocardial infarction. *Cell Transplant.* **2015**, *24*, 1313–1328.

26. Liang, Z.; Yoon, Y.; Votaw, J.; Goodman, M. M.; Williams, L.; Shim, H. Silencing of CXCR4 blocks breast cancer metastasis. *Cancer Res.* **2005**, *65*, 967–971.

27. Chen, Y.; Huang, Y.; Reiberger, T.; Duyverman, A. M.; Huang, P.; Samuel, R.; Hiddingh, L.; Roberge, S.; Koppel, C.; Lauwers, G. Y.; Zhu, A. X.; Jain, R. K.; Duda, D. G. Differential effects of sorafenib on liver versus tumor fibrosis mediated by stromal-derived factor 1 alpha/C-X-C receptor type 4 axisand myeloid differentiation antigen-positive myeloid cell infiltration in mice. *Hepatology* **2014**, *59*, 1435–1447.

28. Matthys, P.; Hatse, S.; Vermeire, K.; Wuyts, A.; Bridger, G.; Henson, G. W.; De Clercq, E.; Billiau, A.; Schols, D. AMD3100, a potent and specific antagonist of the stromal cell-derived factor-1 chemokine receptor CXCR4, inhibits autoimmune joint inflammation in IFN-gamma receptor-deficient mice. *J. Immunol.* **2001**, *167*, 4686–4692.

29. Walter, H. L.; van der Maten, G.; Antunes, A. R.; Wieloch, T.; Ruscher, K. Treatment with AMD3100 attenuates the microglial response and improves outcome after experimental stroke. *J. Neuroinflammation* **2015**, *12*, 24.

30. Ruscher, K.; Kuric, E.; Liu, Y.; Walter, H. L.; Issazadeh-Navikas, S.; Englund, E.; Wieloch, T. Inhibition of CXCL12 signaling attenuates the postischemic immune response and improves functional recovery after stroke. *J. Cereb. Blood Flow Metab.* **2013**, *33*, 1225–1234.

31. Huang, J.; Li, Y.; Tang, Y.; Tang, G.; Yang, G. Y.; Wang, Y. CXCR4 antagonist AMD3100 protects blood-brain barrier integrity and reduces inflammatory response after focal ischemia in mice. *Stroke* **2013**, *44*, 190–197.

32. Jujo, K.; Ii, M.; Sekiguchi, H.; Klyachko, E.; Misener, S.; Tanaka, T.; Tongers, J.; Roncalli, J.; Renault, M. A.; Thorne, T.; Ito, A.; Clarke, T.; Kamide, C.; Tsurumi, Y.; Hagiwara, N.; Qin, G.; Asahi, M.; Losordo, D. W. CXC-chemokine receptor 4 antagonist AMD3100 promotes cardiac functional recovery after

ischemia/reperfusion injury via endothelial nitric oxide synthase-dependent mechanism. *Circulation* **2013**, *127*, 63–73.

33. Liles, W. C.; Broxmeyer, H. E.; Rodger, E.; Wood, B.; Hübel, K.; Cooper, S.; Hangoc, G.; Bridger, G. J.; Henson, G. W.; Calandra, G.; Dale, D. C. Mobilization of hematopoietic progenitor cells in healthy volunteers by AMD3100, a CXCR4 antagonist. *Blood* **2003**, *102*, 2728–2730.

34. DiPersio, J. F.; Micallef, I. N.; Stiff, P. J.; Bolwell, B. J.; Maziarz, R. T.; Jacobsen, E.; Nademanee, A.; McCarty, J.; Bridger, G.; Calandra, G. Phase III prospective randomized double-blind placebo-controlled trial of plerixafor plus granulocyte colony-stimulating factor compared with placebo plus granulocyte colony-stimulating factor for autologous stem-cell mobilization and transplantation for patients with non-Hodgkin's lymphoma. *J. Clin. Oncol.* **2009**, *27*, 4767–4773.

35. (a) Stiff, P.; Micallef, I.; McCarthy, P.; Magalhaes-Silverman, M.; Weisdorf, D.; Territo, M.; Badel, K.; Calandra, G. Treatment with plerixafor in non-Hodgkin's lymphoma and multiple myeloma patients to increase the number of peripheral blood stem cells when given a mobilizing regimen of G-CSF: implications for the heavily pretreated patient. *Biol. Blood Marrow Transplant.* **2009**, *15*, 249–256. (b) MacKenzie, A. R.; Valsecchi, M. E.; Flomenberg, N. The Current Role of Plerixafor in Stem Cell Mobilization for Hematopoietic Stem Cell Transplantation. In *Novel*

Developments in Stem Cell Mobilization; Fruehauf, S., Zeller, W. J., Calandra, G., Eds.; Springer: Boston, MA, 2012; pp 103−131.

36. Devine, S. M.; Flomenberg, N.; Vesole, D. H.; Liesveld, J.; Weisdorf, D.; Badel, K.; Calandra, G.; DiPersio, J. F. Rapid mobilization of CD34+ cells following administration of the CXCR4 antagonist AMD3100 to patients with multiple myeloma and non-Hodgkin's lymphoma. *J. Clin. Oncol.* **2004**, *22*, 1095–1102.

37. Hess, D. A.; Bonde, J.; Craft, T. P.; Wirthlin, L.; Hohm, S.; Lahey, R.; Todt, L. M.; Dipersio, J. F.; Devine, S. M.; Nolta, J. A. Human progenitor cells rapidly mobilized by AMD3100 repopulate NOD/SCID mice with increased frequency in comparison to cells from the same donor mobilized by granulocyte colony stimulating factor. *Biol. Blood Marrow Transplant.* **2007**, *13*, 398–411.

38. Larochelle, A.; Krouse, A.; Metzger, M.; Orlic, D.; Donahue, R. E.; Fricker, S.; Bridger, G.; Dunbar, C. E.; Hematti, P. AMD3100 mobilizes hematopoietic stem cells with long-term repopulating capacity in nonhuman primates. *Blood* **2006**, *107*, 3772–3778.

39. Banerjee, S.; Bentley, P.; Hamady, M.; Marley, S.; Davis, J.; Shlebak, A.; Nicholls, J.; Williamson, D. A.; Jensen, S. L.; Gordon, M.; Habib, N.; Chataway, J. Intra-arterial immunoselected CD34+ stem cells for acute ischemic stroke. *Stem Cells Transl. Med.* **2014**, *3*, 1322–1330.

40. (a) Ichiyama, K.; Yokoyama-Kumakura, S.; Tanaka, Y.; Tanaka, R.; Hirose, K.; Bannai, K.; Edamatsu, T.; Yanaka, M.; Niitani, Y.; Miyano-Kurosaki, N.; Takaku, H.; Koyanagi, Y.; Yamamoto, N. A duodenally absorbable CXC chemokine receptor 4 antagonist, KRH-1636, exhibits a potent and selective anti-HIV-1 activity. *Proc. Natl. Acad. Sci. U. S. A.* **2003**, *100*, 4185–4190. (b) Tamamura, H.; Araki, T.; Ueda, S.; Wang, Z.; Oishi, S.; Esaka, A.; Trent, J. O.; Nakashima, H.; Yamamoto, N.; Peiper, S. C.; Otaka, A.; Fujii, N. Identification of novel low molecular weight CXCR4 antagonists by structural tuning of cyclic tetrapeptide scaffolds. *J. Med. Chem.* **2005**, *48*, 3280–3289. (c) Ueda, S.; Oishi, S.; Wang, Z. X.; Araki, T.; Tamamura, H.; Cluzeau, J.; Ohno, H.; Kusano, S.; Nakashima, H.; Trent, J. O.; Peiper, S. C.; Fujii, N. Structure-activity relationships of cyclic peptide-based chemokine receptor CXCR4 antagonists: disclosing the importance of side-chain and backbone functionalities. *J. Med. Chem.* **2007**, *50*, 192–198. (d) Demmer, O.; Dijkgraaf, I.; Schottelius, M.; Wester, H. J.; Kessler, H. Introduction of functional groups into peptides via N-alkylation. *Org. Lett.* **2008**, *10*, 2015–2018. (e) Thoma, G.; Streiff, M. B.; Kovarik, J.; Glickman, F.; Wagner, T.; Beerli, C.; Zerwes, H. G. Orally bioavailable isothioureas block function of the chemokine receptor CXCR4 in vitro and in vivo. *J. Med. Chem.* **2008**, *51*, 7915–7920. (f) Zhu, A.; Zhan, W.; Liang, Z.; Yoon, Y.; Yang, H.; Grossniklaus, H. E.; Xu, J.; Rojas, M.; Lockwood, M.; Snyder, J.

P.; Liotta, D. C.; Shim, H. Dipyrimidine amines: a novel class of chemokine receptor type 4 antagonists with high specificity. *J. Med. Chem.* **2010**, *53*, 8556–8568. (g) Miller, J. F.; Gudmundsson, K. S.; Richardson, L. D.; Jenkinson, S.; Spaltenstein, A.; Thomson, M.; Wheelan, P. Synthesis and SAR of novel isoquinoline CXCR4 antagonists with potent anti-HIV activity. *Bioorg. Med. Chem. Lett.* **2010**, *20*, 3026–3030. (h) Catalano, J. G.; Gudmundsson, K. S.; Svolto, A.; Boggs, S. D.; Miller, J. F.; Spaltenstein, A.; Thomson, M.; Wheelan, P.; Minick, D. J.; Phelps, D. P.; Jenkinson, S. Synthesis of a novel tricyclic 1,2,3,4,4a,5,6,10b-octahydro-1,10-phenanthroline ring system and CXCR4 antagonists with potent activity against HIV-1. *Bioorg. Med. Chem. Lett.* **2010**, *20*, 2186–2190. (i) Miller, J. F.; Turner, E. M.; Gudmundsson, K. S.; Jenkinson, S.; Spaltenstein, A.; Thomson, M.; Wheelan, P. Novel N-substituted benzimidazole CXCR4 antagonists as potential anti-HIV agents. *Bioorg. Med. Chem. Lett.* **2010**, *20*, 2125–2128. (j) Skerlj, R.; Bridger, G.; McEachern, E.; Harwig, C.; Smith, C.; Wilson, T.; Veale, D.; Yee, H.; Crawford, J.; Skupinska, K.; Wauthy, R.; Yang, W.; Zhu, Y.; Bogucki, D.; Fluri, M. D.; Langille, J.; Huskens, D.; De Clercq, E.; Schols, D. Synthesis and SAR of novel CXCR4 antagonists that are potent inhibitors of T tropic (X4) HIV-1 replication. *Bioorg. Med. Chem. Lett.* **2011**, *21*, 262–266. (k) Wu, C. H.; Chang, C. P.; Song, J. S.; Jan, J. J.; Chou, M. C.; Wu, S. H.; Yeh, K. C.; Wong, Y. C.; Hsieh, C. J.; Chen, C. T.; Kao, T. T.; Wu, S. Y.; Yeh, C. F.;

Tseng, C. T.; Chao, Y. S.; Shia, K. S. Discovery of novel stem cell mobilizers that target the CXCR4 receptor. *ChemMedChem* **2012**, *7*, 209–212. (l) Truax, V. M.; Zhao, H.; Katzman, B. M.; Prosser, A. R.; Alcaraz, A. A.; Saindane, M. T.; Howard, R. B.; Culver, D.; Arrendale, R. F.; Gruddanti, P. R.; Evers, T. J.; Natchus, M. G.; Snyder, J. P.; Liotta, D. C.; Wilson, L. J. Discovery of tetrahydroisoquinoline-based CXCR4 antagonists. *ACS Med. Chem. Lett.* **2013**, *4*, 1025–1030. (m) Mooring, S. R.; Gaines, T.; Liang, Z.; Shim, H. Synthesis of pyridine derivatives as potential antagonists of chemokine receptor type 4. *Heterocycl. Commun.* **2014**, *20*, 149–153. (n) Zachariassen, Z. G.; Thiele, S.; Berg, E. A.; Rasmussen, P.; Fossen, T.; Rosenkilde, M. M.; Våbenø, J.; Haug, B. E. Design, synthesis, and biological evaluation of scaffold-based tripeptidomimetic antagonists for CXC chemokine receptor 4 (CXCR4). *Bioorg. Med. Chem.* **2014**, *22*, 4759–4769. (o) Nomura, W.; Koseki, T.; Ohashi, N.; Mizuguchi, T.; Tamamura, H. Trivalent ligands for CXCR4 bearing polyproline linkers show specific recognition for cells with increased CXCR4 expression. *Org. Biomol. Chem.* **2015**, *13*, 8734–8739. (p) Curreli, F.; Kwon, Y. D.; Zhang, H.; Scacalossi, D.; Belov, D. S.; Tikhonov, A. A.; Andreev, I. A.; Altieri, A.; Kurkin, A. V.; Kwong, P. D.; Debnath, A. K. Structure-based design of a small molecule CD4-antagonist with broad spectrum anti-HIV-1 activity. *J. Med. Chem.* **2015**, *58*, 6909−6927. (q) Zhan, Y.; Zhang, H.; Li, J.; Zhang, Y.; Zhang, J.; He,

L. A novel biphenyl urea derivate inhibits the invasion of breast cancer through the modulation of CXCR4. *J. Cell. Mol. Med.* **2015**, *19*, 1614−1623. (r) Våbenø, J.; Haug, B. E.; Rosenkilde, M. M. Progress toward rationally designed small-molecule peptide and peptidomimetic CXCR4 antagonists. *Future Med. Chem.* **2015**, *7*, 1261–1283. (s) Zhao, H.; Prosser, A. R.; Liotta, D. C.; Wilson, L. J. Discovery of novel N-aryl piperazine CXCR4 antagonists. *Bioorg. Med. Chem. Lett.* **2015**, *25*, 4950–4955. (t) Cox, B. D.; Prosser, A. R.; Sun, Y.; Li, Z.; Lee, S.; Huang, M. B.; Bond, V. C.; Snyder, J. P.; Krystal, M.; Wilson, L. J.; Liotta, D. C. Pyrazolo-piperidines exhibit dual inhibition of CCR5/CXCR4 HIV entry and reverse transcriptase. *ACS Med. Chem. Lett.* **2015**, *6*, 753−757. (u) Mishra, R. K.; Shum, A. K.; Platanias, L. C.; Miller, R. J.; Schiltz, G. E. Discovery and characterization of novel small-molecule CXCR4 receptor agonists and antagonists. *Sci. Rep.* **2016**, *6*, 30155. (v) Puig de la Bellacasa, R.; Gibert, A.; Planesas, J. M.; Ros-Blanco, L.; Batllori, X.; Badía, R.; Clotet, B.; Esté, J.; Teixidóa, J.; Borrell, J. I. Nitrogen positional scanning in tetramines active against HIV-1 as potential CXCR4 inhibitors. *Org. Biomol. Chem.* **2016**, *14*, 1455–1472. (w) Bai, R.; Liang, Z.; Yoon, Y.; Liu, S.; Gaines, T.; Oum, Y.; Shi, Q.; Mooring, S. R.; Shim, H. Symmetrical bis-tertiary amines as novel CXCR4 inhibitors. *Eur. J. Med. Chem.* **2016**, *118*, 340–350. (x) Gaines, T.; Camp, D.; Bai, R.; Liang, Z.; Yoon, Y.; Shim, H.; Mooring, S. R. Synthesis and evaluation of 2,5 and

2,6 pyridine-based CXCR4 inhibitors. *Bioorg. Med. Chem. Lett.* **2016**, *24*, 5052–5060.

41. (a) Wu, B.; Chien, E. Y. T.; Mol, C. D.; Fenalti, G.; Liu, W.; Katritch, V.; Abagyan, R.; Brooun, A.; Wells, P.; Bi, F. C.; Hamel, D. J.; Kuhn, P.; Handel, T. M.; Cherezov, V.; Stevens, R. C. Structures of the CXCR4 chemokine GPCR with small-molecule and cyclic peptide antagonists. *Science* **2010**, *330*, 1066–1071. (b) Qin, L.; Kufareva, I.; Holden, L. G.; Wang, C.; Zheng, Y.; Zhao, C.; Fenalti, G.; Wu, H.; Han, G. W.; Cherezov, V.; Abagyan, R.; Stevens, R. C.; Handel, T. M. Crystal structure of the chemokine receptor CXCR4 in complex with a viral chemokine. *Science* **2015**, *347*, 1117–1122.
42. Zhu, L.; Zhao, Q.; Wu, B. Structure-based studies of chemokine receptors. *Curr. Opin. Struct. Biol.* **2013**, *23*, 539–546.
43. Shia, K. S.; Jan, J. J.; Tsou, L. K.; Chen, C. T.; Chao, Y. S. Heterocyclic Compounds and Use Thereof. U.S. Patent 0,083,369, March 24, 2016.
44. Matsuoka, S.; Ebihara, Y.; Xu, M.; Ishii, T.; Sugiyama, D.; Yoshino, H.; Ueda, T.; Manabe, A.; Tanaka, R.; Ikeda, Y.; Nakahata, T.; Tsuji, K. CD34 expression on long-term repopulating hematopoietic stem cells changes during developmental stages. *Blood* **2001**, *97*, 419–425.

45. Arndt, K.; Grinenko, T.; Mende, N.; Reichert, D.; Portz, M.; Ripich, T.; Carmeliet, P.; Corbeil, D.; Waskow, C. CD133 is a modifier of hematopoietic progenitor frequencies but is dispensable for the maintenance of mouse hematopoietic stem cells. *Proc. Natl. Acad. Sci. U. S. A.* **2013**, *110*, 5582–5587.

46. Lee, H. J.; Choi, C. W.; Kim, E. K.; Kim, H. S.; Kim, B. I.; Choi, J. H. Granulocyte colony-stimulating factor reduces hyperoxia-induced alveolarization inhibition by increasing angiogenic factors. *Neonatology* **2012**, *101*, 278–284.

47. Westvik, T. S.; Fitzgerald, T. N.; Muto, A.; Maloney, S. P.; Pimiento, J. M.; Fancher, T. T.; Magri, D.; Westvik, H. H.; Nishibe, T.; Velazquez, O. C.; Dardik, A. Limb ischemia after iliac ligation in aged mice stimulates angiogenesis without arteriogenesis. *J. Vasc. Surg.* **2009**, *49*, 464–473.

48. (a) Broxmeyer, H. E.; Orschell, C. M.; Clapp, D. W.; Hangoc, G.; Cooper, S.; Plett, P. A.; Liles, W. C.; Li, X.; Graham-Evans, B.; Campbell, T. B.; Calandra, G.; Bridger, G.; Dale, D. C.; Srour, E. F. Rapid mobilization of murine and human hematopoietic stem and progenitor cells with AMD3100, a CXCR4 antagonist. *J. Exp. Med.* **2005**, *201*, 1307–1318. (b) Yin, Y.; Huang, L.; Zhao, X.; Fang, Y.; Yu, S.; Zhao, J.; Cui, B. AMD3100 mobilizes endothelial progenitor cells in mice, but inhibits its biological functions by blocking an autocrine/paracrine regulatory loop of stromal cell derived factor-1 in vitro. *J. Cardiovasc. Pharmacol.* **2007**, *50*, 61–67.

49. Ward, P. A. Leukotaxis and leukotactic disorders. A review. *Am. J. Pathol.* **1974**, *77*, 520–538.

50. The pharmacology and toxicology of plerixafor (NDA: 022311, p.43) https://www.accessdata.fda.gov/drugsatfda_docs/nda/2008/022311s000_PharmR.pdf. (accessed Dec 15, 2008)

51. Baell, J. B.; Holloway, G. A. New substructure filters for removal of pan assay interference compounds (PAINS) from screening libraries and for their exclusion in bioassays. *J. Med. Chem.* **2010**, *53*, 2719–2740.

52. Brooks, B. R.; Brooks, C. L. 3rd.; Mackerell, A. D. Jr.; Nilsson, L.; Petrella, R. J.; Roux, B.; Won, Y.; Archontis, G.; Bartels, C.; Boresch, S.; Caflisch, A.; Caves, L.; Cui, Q.; Dinner, A. R.; Feig, M.; Fischer, S.; Gao, J.; Hodoscek, M.; Im, W.; Kuczera, K.; Lazaridis, T.; Ma, J.; Ovchinnikov, V.; Paci, E.; Pastor, R. W.; Post, C. B.; Pu, J. Z.; Schaefer, M.; Tidor, B.; Venable, R. M.; Woodcock, H. L.; Wu, X.; Yang, W.; York, D. M.; Karplus, M. CHARMM: the biomolecular simulation program. *J. Comput. Chem.* **2009**, *30*, 1545–1614.

53. Berendsen, H. J. C.; Vanderspoel, D.; Vandrunen, R. GROMACS: a message-passing parallel molecular-dynamics implementation. *Comp. Phys. Comm.* **1995**, *91*, 43–56.

54. Schuttelkopf, A. W.; van Aalten, D. M. PRODRG: a tool for high-throughput crystallography of protein-ligand complexes. *Acta Crystallogr. D Biol. Crystallogr.* **2004**, *60*, 1355–1363.

55. Chiu, S. W.; Pandit, S. A.; Scott, H. L.; Jakobsson, E. An improved united atom force field for simulation of mixed lipid bilayers. *J. Phys. Chem. B* **2009**, *113*, 2748–2763.

56. Hess, B.; Bekker, H.; Berendsen, H. J. C.; Fraaije, J. G. E. M. LINCS: a linear constraint solver for molecular simulations. *J. Comp. Chem.* **1997**, *18*, 1463–1472.

Table of Contents Graphic